

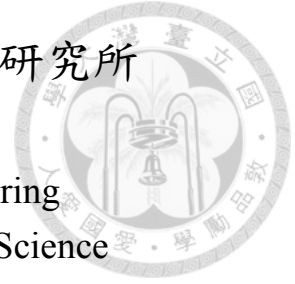
國立臺灣大學電機資訊學院電信工程研究所

碩士論文

Graduate Institute of Communication Engineering  
College of Electrical Engineering and Computer Science

National Taiwan University

Master Thesis



擴散型分子通訊之編碼距離函式與其應用

Coding Distance Function for

Diffusion-based Molecular Communication and Its Application

柯品仔

Pin-Yu Ko

指導教授：葉丙成 博士

Advisor: Ping-Cheng Yeh, Ph.D.

中華民國 103 年 7 月

July, 2014

國立臺灣大學（碩）博士學位論文  
口試委員會審定書

擴散型分子通訊之編碼距離函式與其應用  
Coding Distance Function for Diffusion-based Molecular  
Communication and Its Application

本論文係柯品仔君（學號 R01942049）在國立臺灣大學電信工程  
學研究所完成之碩（博）士學位論文，於民國 103 年 7 月 16 日承下  
列考試委員審查通過及口試及格，特此證明

口試委員：

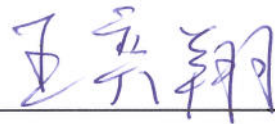


（簽名）

（指導教授）







所 長



（簽名）





## 致謝

研究路上最感謝的莫過於葉丙成老師，教學的熱忱讓我們重新思考人生的方向；大三下專題課的場景仿若昨日，轉眼進實驗室已四年。非常感謝李佳翰老師給我很多建議，教我用更廣的視野看待研究，並將目標放得更高遠。謝謝彥奇學長的指導、令三學長的提攜、泓瑞學長的支持，感謝同在分子通訊組的維安，謝謝你在我遇到瓶頸時給我新的想法；謝謝夥伴們駿挺、昀鋒、博凱、柏均一同在學術上努力。

515 為生活帶來許多歡笑，謝謝李俊時時分享有趣的新事物、偉軒辦了好多活動、穴宇無私地幫助大家，也謝謝 515 之友品萱一起討論未來的方向。謝謝柏希有好多點讓我們嗆、皓中和我們一起在實驗室奮鬥。謝謝上屆學長帶給 515 的無限樂趣，Kenji 總是帥帥地搞笑、植鈺邊看 AKB48 邊教我寫程式、Golo 和美麗的 Celeste 閃亮亮出場、謝謝曄智的關懷與陪伴。

研究所的日子裡，除了實驗室外也想感謝認識十年的高中好友，從遠方支持的花花、一起開心上課的方克、時常聊天的慧婷與家蓉，互相打氣的小依和丁丁。謝謝從大學以來童語六六團本、湘涵和于婷，還有共同修課的劭安、關心我的綠豆。學校外的 StorySense 是我的避風港，尤其是湘庭和芳瑜的鼓勵，讓我在實習時得到成就感和溫暖的力量。感謝 MS 新夥伴的互相扶持，讓我能開心地大笑做自己。

感謝家人義無反顧地成為我的後盾，一路上辛苦為家庭付出的媽媽、給我不同角度建議的爸爸和非常照顧我的弟弟！我愛你們！自入學起便翹首期盼完成學位，但真正達成的這一刻卻伴隨新的責任與方向。一路走來需要感謝者眾，希望這些字句能訴盡我真摯的謝意。





## 中文摘要

近年來奈米技術發展迅速，可被應用於生醫、軍事、工業等領域。由於單一個奈米機器的運算能力有限，要達成規模較大的任務需仰賴於多個奈米機器間的溝通。如果要採用傳統的電磁波作為通訊方式，則必須要在每一個奈米機器上裝載天線，然而考慮到奈米機器的尺寸較小，此方案的可行性較低。因此，聲波、奈米碳管和分子通訊等新的奈米通訊技術陸續被提出以解決奈米機器溝通的問題。其中，分子通訊因其生物相容性高，是近年來發展迅速、並被認為是最有可能被實現的奈米通訊技術。我們採用的擴散型分子通訊是一種利用分子在液態溶液中自由運動傳遞訊息的分子通訊方式。由於擴散型分子的自由運動性質，分子從傳送端抵達接收端的時間是隨機的，此性質會造成訊息的傳遞錯誤。因此，我們使用通道編解碼以增加擴散型分子通訊的可靠度。在傳統電磁通訊上，我們常用極大化最小的碼字 (codeword) 間的漢明距離 (Hamming distance) 來設計通道編碼及解碼。但由於分子通訊的傳遞方式與傳統的電磁波通訊在本質上有很大的差異，傳統通訊上常用的距離將不再適用。因此我們建立了兩種適合擴散型分子通訊的編碼距離函式：「機率型距離函式」與「位元型距離函式」。數據顯示，以提出的這兩種編碼距離函式進行最小距離解碼，其符元錯誤率 (symbol error rate) 近乎最佳解碼方式。本論文的貢獻為在擴散型分子通訊中提出更進一步的通道編碼方式。





# Abstract

Molecular communication is an emerging and promising approach to communications between nanoscale devices due to its biocompatibility nature. In diffusion-based molecular communications, molecules as information carriers diffuse randomly in the fluid medium. Due to the random movements, molecules may arrive at the receiver at random times, resulting in detection errors. Applying channel coding is thus crucial for enhancing the transmission reliability. The paradigm of maximizing the minimum Hamming distance among the codewords has long been used in electromagnetic communication. However, for molecular communication environments, existing distances may be unsuitable because the nature of molecular communication differs from electromagnetic communication. We propose two categories of distance functions - the *probability-based distance function* and the *pattern-based distance function* - tailored for diffusion-based molecular communications. We apply minimum distance decoding rules with the proposed distance functions to diffusion-based molecular communication systems. The numerical results show that these decoding rules are near-optimal. The channel coding application in diffusion-based molecular communication is advanced through this thesis.



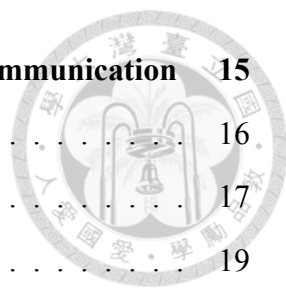




# Contents

口試委員會審定書	i
致謝	iii
中文摘要	v
Abstract	vii
Contents	ix
List of Figures	xi
List of Tables	xv
<b>1 Introduction</b>	<b>1</b>
1.1 Molecular Communication . . . . .	2
1.2 Diffusion-based Molecular Communication . . . . .	3
1.3 Distance Function . . . . .	4
<b>2 Diffusion-based Molecular Communication</b>	<b>5</b>
2.1 System Model . . . . .	5
2.1.1 Active Transport via Brownian Motion with Drift . . . . .	6
2.1.2 Passive Transport via Brownian Motion . . . . .	8
2.2 Modulation of Diffusion-based Molecular Communication . . . . .	9
2.3 Channel Characteristics . . . . .	11
2.4 Channel Coding for Diffusion-based Molecular Communication . . . . .	12

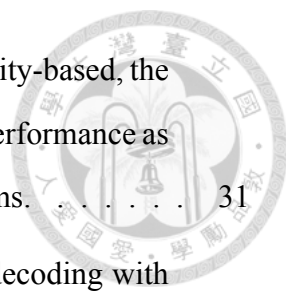
<b>3</b>	<b>Coding Distance Functions for Diffusion-based Molecular Communication</b>	<b>15</b>
3.1	Hamming Distance . . . . .	16
3.2	Notations and Preliminaries . . . . .	17
3.3	Optimal Distance Function for One-shot Transmission . . . . .	19
3.4	Probability-based Distance Function . . . . .	20
3.5	Pattern-based Distance Function . . . . .	21
<b>4</b>	<b>Channel Coding Design for On-off Keying Modulation</b>	<b>25</b>
4.1	On-off Keying Modulation . . . . .	25
4.2	Minimum Distance Decoding for On-off Keying Modulation . . . . .	26
4.3	Numerical Results . . . . .	26
4.3.1	Active Transport via Brownian Motion with Drift . . . . .	27
4.3.2	Passive Transport via Brownian Motion . . . . .	31
<b>5</b>	<b>Channel Coding Design for Synchronous Type-based Modulation</b>	<b>37</b>
5.1	Synchronous Type-Based Modulation . . . . .	37
5.2	Minimum Distance Decoding for Synchronous Type-based Modulation . . . . .	38
5.3	Numerical Results . . . . .	40
5.3.1	Active Transport via Brownian Motion with Drift . . . . .	40
5.3.2	Passive Transport via Brownian Motion . . . . .	44
<b>6</b>	<b>Conclusions and Future Research</b>	<b>49</b>
	<b>Bibliography</b>	<b>51</b>



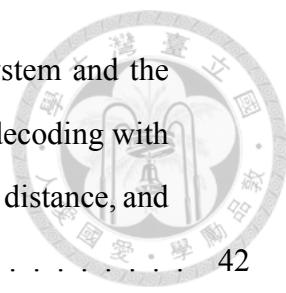


# List of Figures

2.1	End-to-end model for diffusion-based molecular communications. . . . .	6
2.2	The PDF of the first hitting time for active transport defined in (2.2) with $D = 10^{-6}$ cm <sup>2</sup> /s, $d = 20$ $\mu$ m and $v = 2$ $\mu$ m/s. . . . .	7
2.3	The PDF of the first hitting time for passive transport defined in (2.5) with $D = 10^{-6}$ cm <sup>2</sup> /s and $d = 20$ $\mu$ m. . . . .	9
2.4	The PDF comparison of the first hitting time for active and passive transport defined in (2.2) and (2.5). . . . .	10
2.5	Coding scheme illustration for OOK and TM systems. A [4, 2] block code with codebook $\{(0, 0, 0, 1), (0, 0, 1, 0), (0, 1, 1, 1), (1, 0, 1, 1)\}$ is used. In the OOK system, a molecule is released when the coded data bit is ‘1’. In the type-based modulation system, molecule types $A$ , $B$ , and $C$ represent data bits ‘01’, ‘10’, and ‘11’, respectively, and a silence represents ‘00’. . . . .	13
3.1	Example of calculating the pattern-based distance. . . . .	22
4.1	Illustration of the on-off keying (OOK) modulation scheme. . . . .	26
4.2	SER distribution under different decoding rules for OOK systems with $T = 100$ s. The codebooks are indexed by the order of descending SER using the optimal decoding rule. . . . .	28
4.3	Comparison of SER performances for the uncoded OOK system and the coded OOK systems employing optimal decoding rule, MD decoding with probability-based distance, MD decoding with pattern-based distance, and MD decoding with Hamming distance. . . . .	30



4.4	The amount of codebooks decoding by MD with the probability-based, the pattern-based, and the Hamming distance having the same performance as the optimal decoding rule under different $T$ for OOK systems. . . . .	31
4.5	The amount of codebook performing the best among MD decoding with the probability-based, the pattern-based, and the Hamming distance under different $T$ for OOK systems. . . . .	32
4.6	SER distribution under different decoding rules for OOK systems with $T = 100$ s. The codebooks are indexed by the order of descending SER using the optimal decoding rule. . . . .	33
4.7	Comparison of SER performances for the uncoded OOK system and the coded OOK systems employing optimal decoding rule, MD decoding with probability-based distance, MD decoding with pattern-based distance, and MD decoding with Hamming distance. . . . .	35
4.8	The amount of codebooks decoding by MD with the probability-based, the pattern-based, and the Hamming distance having the same performance as the optimal decoding rule under different $T$ for OOK systems. . . . .	36
4.9	The amount of codebook performing the best among MD decoding with the probability-based, the pattern-based, and the Hamming distance under different $T$ for OOK systems. . . . .	36
5.1	Demonstration of the minimum distance decoding process for the type-based modulation systems. The TM system is decomposed into three OOK sub-systems. Molecule types $A$ , $B$ , and $C$ represent data bits ‘01’, ‘10’, and ‘11’, respectively, and a silence represents ‘00’. We use the $[4, 2]$ block code with codebook $\{(0, 0, 0, 1), (0, 0, 1, 0), (0, 1, 1, 1), (1, 0, 1, 1)\}$ for example. . . . .	39
5.2	SER distribution under different decoding rules for TM systems with $T = 100$ s. The codebooks are indexed by the order of descending SER using the optimal decoding rule. . . . .	41



5.3 Comparison of SER performances for the uncoded TM system and the coded TM systems employing optimal decoding rule, MD decoding with probability-based distance, MD decoding with pattern-based distance, and MD decoding with Hamming distance. . . . . 42

5.4 The amount of codebooks decoding by MD with the probability-based, the pattern-based, and the Hamming distance having the same performance as the optimal decoding rule under different  $T$  for TM systems. . . . . 43

5.5 The amount of codebook performing the best among MD decoding with the probability-based, the pattern-based, and the Hamming distance under different  $T$  for TM systems. . . . . 44

5.6 SER distribution under different decoding rules for TM systems with  $T = 100$  s. The codebooks are indexed by the order of descending SER using the optimal decoding rule. . . . . 45

5.7 Comparison of SER performances for the uncoded TM system and the coded TM systems employing optimal decoding rule, MD decoding with probability-based distance, MD decoding with pattern-based distance, and MD decoding with Hamming distance. . . . . 46

5.8 The amount of codebooks decoding by MD with the probability-based, the pattern-based, and the Hamming distance performing having the same performance as the optimal decoding rule under different  $T$  for TM systems. 47

5.9 The amount of codebook performing the best among MD decoding with the probability-based, the pattern-based, and the Hamming distance under different  $T$  for TM systems. . . . . 48





# List of Tables

1.1	Main differences between traditional communication and molecular communication [1, 12] . . . . .	3
4.1	The best performance codebook and the corresponding decoding regions under the optimal decoding rule and the probability-based distance. . . .	29
4.2	The best performance codebook and the corresponding decoding regions under the optimal decoding rule. . . . .	34







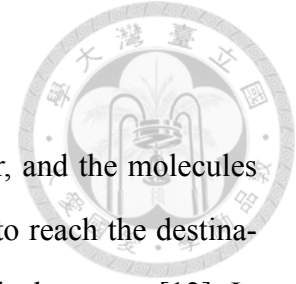
# Chapter 1

## Introduction

Nanotechnology promises new solutions in biomedical, industrial, environmental and military fields [1–6]. Nanomachines are devices in nanoscale which are able to sense, compute, and actuate [7]. Nevertheless, their limited sizes and capabilities force them to cooperate with others in order to perform more complicated tasks. Nanonetwork - interconnecting and exchanging information between several nanomachines - can expand the capability of a single nanomachine [1, 8]. However, communicating between nanomachines is a challenging task. In communication technology, existing forms of transmitting information are mostly based on electromagnetic propagation. However, the antenna sizes are too large and the computational requirements are too high for nanomachines.

Different communication approaches come out for nanonetworks, including *acoustic*, *nano-electromagnetic*, *nano-mechanical*, and *molecular communication*. Acoustic communication uses acoustic energy (i.e. pressure variations) to encode. In nano-electromagnetic communication, the transmission is based on electromagnetic waves resonating carbon nanotube or using graphene-based nanoantennas as radiators [9, 10]. Nano-mechanical communication transmits information through mechanical contact between the transmitter and the receiver. Molecular communication uses molecules as the carrier between transmitters and receivers. Among the existing approaches to communicating between nanomachines, molecular communication is considered to be the most promising solution due to its biocompatibility nature [1, 11].

## 1.1 Molecular Communication



Molecular communication uses molecules as information carrier, and the molecules can either follow specific path or propagate within fluidic medium to reach the destination [1]. Molecular communication is highly compatible with biological systems [12]. In biology, molecular communication can be employed over short-range (nm scale) communication, mid-range ( $\mu\text{m}$  to cm scale) communication, or long-range (cm to m scale) communication [13, 14]. For example, neurotransmitters transmit calcium ions to diffuse freely in fluidic medium to communicate over short-range communication; inside cell motor proteins can actively transport vesicles along the rail molecules over mid-range communication; and hormones are transported by blood flow over long-range with active transport with drift (blood flow from the heart) [7, 15].

Molecular communication differs from the well-known traditional electromagnetic communication in many aspects. In molecular communication, the information carriers are molecules which have to be physically transported from the transmitter to the receiver. Besides, the diffusion processes of the molecules are stochastic and depend on the environmental conditions, such as the type of medium and the temperature. The propagation speed is much slower than the electromagnetic communication, where the electromagnetic waves are propagated with light speed. The noise in traditional communication is generated by undesired electrical disturbance of the information signal. While in molecular communication, noise can be originated from the overlap with molecular signals, affecting the molecule concentration level sensed by the receiver, or from undesired chemical reaction occurring between information molecules and other molecules in the environment, making the molecule carriers unable to react with or bond to the receiver [1].

Nevertheless, the energy consumption is lower in molecular communication than traditional communication because most of the processes are chemically driven. In traditional communication, the communication processes consume electrical power that is obtained from batteries or from external sources such as electromagnetic induction. The main differences between traditional communication and molecular communication are shown in Table 1.1 [1, 12]. Due to the significant difference between the molecular communication

and the traditional electromagnetic communication, we have to consider new paradigm for applying conventional communication methodologies to molecular communication.

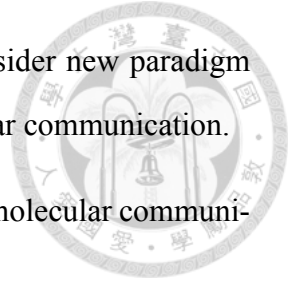


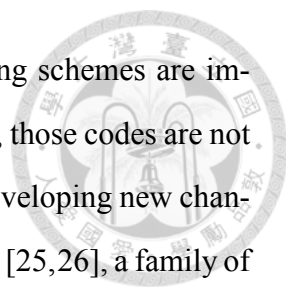
Table 1.1: Main differences between traditional communication and molecular communication [1, 12]

Communication	Traditional	Molecular
Communication carrier	Electromagnetic wave	Molecule
Signal type	Electronic and optical (Electromagnetic)	Chemical
Propagation speed	Light speed	Extremely low
Medium conditions	Wired: Almost immune Wireless: Affect communication	Affect communication
Noise	Electromagnetic fields and signals	Particles and molecules in medium
Encoded information	Voice, text and video	Phenomena, chemical states or processes
Other features	High energy consumption Accurate communication	Low energy consumption Stochastic communication High biocompatibility

## 1.2 Diffusion-based Molecular Communication

Molecular communication can be implemented by transmitting molecules through diffusion, molecular motor, or gap junction [1]. In this thesis, we focus on diffusion-based molecular communication, where molecules rely on the laws of particle diffusion rather than specific path to reach the destination [16]. Each molecule released by the transmitter follows the random-walk diffusion mechanism [17–19] and reaches the receiver according to certain probability laws [20]. The calcium signaling, which plays an important role in many critical biological functions such as the brain-nerve system or the heart functioning in human bodies, is an example of diffusion-based molecular communication [21, 22].

Recent researches on evaluating and bounding the achievable information rate (i.e., channel capacity) for diffusion-based molecular communication under different scenarios have been conducted [18, 19, 23, 24]. In modern wireless communication, to approach the channel capacity, advanced channel coding schemes, e.g., turbo codes and low-density parity-check (LDPC) codes, are often applied. Nevertheless, due to the limited size and



limited computational power of a nanomachine, such complex coding schemes are impractical to be implemented in molecular communication. In addition, those codes are not guaranteed to perform well under the diffusion channel. Therefore, developing new channel codes for molecular communication becomes an important task. In [25,26], a family of channel codes for diffusion-based molecular communication, called intersymbol interference (ISI)-free codes, are explored. These codes effectively improve the communication reliability while keeping the decoding complexity low. However, a general principle of designing a reliable channel code for diffusion-based molecular communication is still an open question.

### 1.3 Distance Function

An approach to tackling this problem is through exploring *distance functions* for decoding under minimum distance (MD.) A well-known example of a distance function is the Hamming distance. Due to the inherent discrepancy between diffusion channels and wireless communication channels, proper distance functions for molecular communication are expected to be different from that for wireless communication. Therefore, new distance functions need to be proposed. In this thesis, we propose two distance functions - the *probability-based distance function* and the *pattern-based distance function* - that are suitable for diffusion channels in molecular communication. With the proposed distance functions, we then investigate the MD decoding. Simulations are conducted to evaluate the effectiveness of the proposed distance functions.

The rest of this thesis is organized as follows. In Chapter 2, we describe the end-to-end system model, the modulation schemes, and the channel coding scenarios. In Chapter 3, we introduce the distance functions for diffusion-based molecular communication. The channel code design and the numerical results for on-off keying and synchronous type-based modulation are presented in Chapter 4 and 5, respectively. Finally the conclusion is made in Chapter 6.



## Chapter 2

# Diffusion-based Molecular Communication

In this chapter, we first describe the end-to-end system and the channel model for both diffusion-based active transport and passive transport. The modulation techniques for the diffusion-based molecular communication are introduced. The channel characteristics and the channel coding schemes considered in this thesis are then presented.

### 2.1 System Model

Fig. 2.1 shows the end-to-end model of the diffusion-based molecular communication system considered in this thesis. Since the environment is assumed to be isotropic [27], we consider a one-dimensional (1-D) diffusion channel to simplify the analysis, and some assumptions are listed as follows. The transmitter and the receiver are separated by a distance  $d$  with fixed locations, and they are assumed to be zero volume. The molecules, used as information carriers, have the same radius  $r$ , and diffuse from the transmitter to the receiver in fluidic environment with diffusion coefficient  $D$ . The molecules will be perfectly absorbed and removed from the fluid media when they reach the receiver. From fluid mechanics, the diffusion coefficient  $D$  is given by [28]

$$D = \frac{k_B T_a}{6\pi r \eta}, \quad (2.1)$$

where  $k_B$  is the Boltzmann constant,  $T_a$  is the absolute temperature,  $r$  is the molecule radius, and  $\eta$  is the viscosity coefficient whose value depends on the liquid type and its temperature.

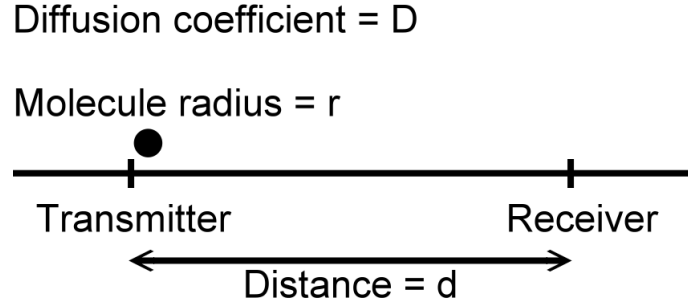
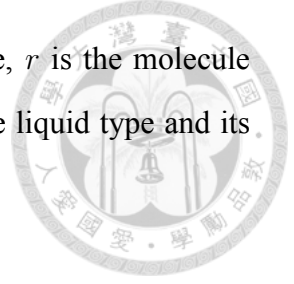


Figure 2.1: End-to-end model for diffusion-based molecular communications.

Considering the channel for diffusing particles, we can divide the diffusion-based molecular communication into two main propagation schemes: active transport, and passive transport [29]. In active transport, the particles, which carry information, propagate from the transmitter to the receiver with external drift generated from molecular motors or external devices such as a syringe pump or a heart which generates the blood flow. In passive transport, the particles propagate to the receiver by diffusing in the fluidic medium without external energy. The active transport achieves higher information rates compared to the passive transport with simple Brownian motions, but introducing drift would require the existence of an external device [15]. Therefore, we consider both the active and passive transport in this thesis to cover the whole scenario of diffusion-based molecular communication.

### 2.1.1 Active Transport via Brownian Motion with Drift

The molecule movements of active transport are modeled as independent Brownian motions with a positive drift velocity  $v$  [18, 19]. The traveling time  $T_s$  ( $> 0$ ) from the transmitter to the receiver of each released molecule, i.e., the *first hitting time*, follows the inverse Gaussian (IG) distribution [30]. The probability density function (PDF) of an IG distribution is [31]

$$f_{IG}(t_s) = \sqrt{\frac{\lambda}{2\pi t_s^3}} \exp\left(-\frac{\lambda(t_s - \mu)^2}{2\mu^2 t_s}\right), \quad (2.2)$$

where  $\mu = \frac{d}{v}$  is the mean first hitting time and  $\lambda = \frac{2d^2}{D}$  is the shape parameter. The cumulative distribution function (CDF) is

$$F_{IG}(t_s) = \Phi\left(\sqrt{\frac{\lambda}{t_s}}\left(\frac{t_s}{\mu} - 1\right)\right) + \exp\left(\frac{2\lambda}{\mu}\right)\Phi\left(-\sqrt{\frac{\lambda}{t_s}}\left(\frac{t_s}{\mu} + 1\right)\right), \quad (2.3)$$

where  $\Phi(\cdot)$  is the standard normal distribution CDF defined as  $\Phi(x) = \frac{1}{\sqrt{2\pi}} \int_{-\infty}^x e^{-y^2/2} dy$ .

The peak probability density of  $T_s$  for active transport happens at

$$\hat{t}_s = \mu \left[ \left(1 + \frac{9\mu^2}{4\lambda^2}\right)^{\frac{1}{2}} - \frac{3\mu}{2\lambda} \right]. \quad (2.4)$$

The variance of  $T_s$  is  $\frac{\mu^3}{\lambda}$ .

In Fig 2.2, we show a PDF example of an IG distribution with parameters based on the calcium signaling [32] by setting the diffusion coefficient  $D = 10^{-6} \text{ cm}^2/\text{s}$ , the distance between the transmitter and the receiver  $d = 20 \text{ }\mu\text{m}$ , and we set the drift velocity to be  $v = 2 \text{ }\mu\text{m/s}$  to have average first hitting time  $10 \text{ s}$ . We can see from Fig 2.2 that the maximum probability density (0.2806) occurs at  $T_s = 0.6637 \text{ s}$ , which is in accordance with (2.4).

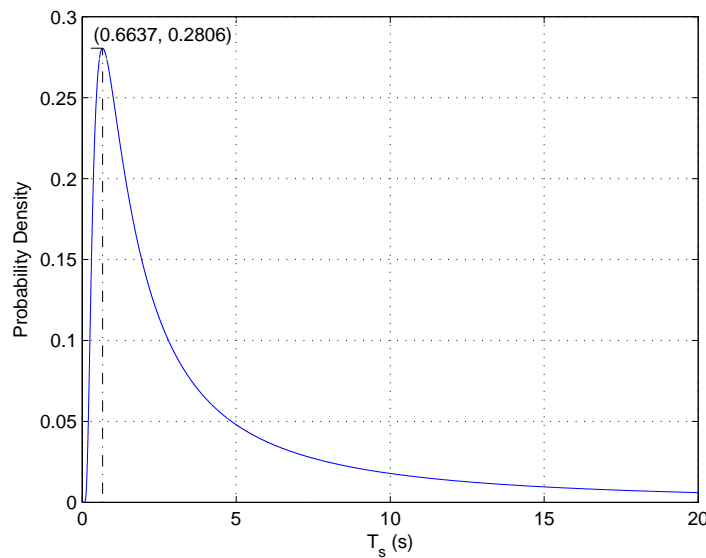
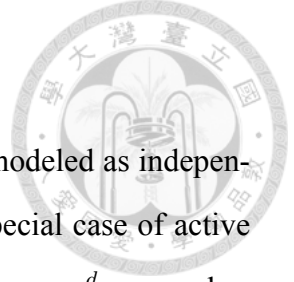


Figure 2.2: The PDF of the first hitting time for active transport defined in (2.2) with  $D = 10^{-6} \text{ cm}^2/\text{s}$ ,  $d = 20 \text{ }\mu\text{m}$  and  $v = 2 \text{ }\mu\text{m/s}$ .





## 2.1.2 Passive Transport via Brownian Motion

The passive transport movements of the released molecules are modeled as independent Brownian motions. Passive transport can be considered as a special case of active transport with zero drift velocity. In this case, the mean first hitting time  $\mu = \frac{d}{v}$  approaches infinity, and the distribution becomes a Lévy distribution. The PDF of the first hitting time  $T_s (> 0)$  is [33]

$$f_L(t_s) = \frac{d}{2\sqrt{D\pi t_s^3}} \cdot \exp\left(-\frac{d^2}{4Dt_s}\right), \quad (2.5)$$

and the CDF of  $T_s$  is [34]

$$F_L(t_s) = \frac{2}{\sqrt{2\pi}} \int_{\frac{d}{\sqrt{2Dt_s}}}^{\infty} e^{-y^2/2} dy = 2Q\left(\frac{d}{\sqrt{2Dt_s}}\right), \quad (2.6)$$

where  $Q(\cdot)$  is the standard  $Q$ -function defined as  $Q(x) = \frac{1}{\sqrt{2\pi}} \int_x^{\infty} e^{-y^2/2} dy = 1 - \Phi(x)$ .

The peak probability density of  $T_s$  for passive transport happens at

$$\hat{t}_s = \frac{d^2}{6D}. \quad (2.7)$$

The mean and the variance of  $T_s$  are both infinite in the case of passive transport.

Again, we show a PDF example for passive transport in Fig 2.3 with parameters  $D = 10^{-6} \text{ cm}^2/\text{s}$  and  $d = 20 \text{ }\mu\text{m}$  according to the calcium signaling [32]. The maximum probability density (0.2313) occurs at  $T_s = 0.6667 \text{ s}$ , which fits the peak probability density equation (2.7).

In order to have a deeper look into the active and the passive transport, we plot the PDFs with log scale for both the active and passive transport in Fig. 2.4 with parameters mentioned as above:  $D = 10^{-6} \text{ cm}^2/\text{s}$  and  $d = 20 \text{ }\mu\text{m}$  for both transport, and  $v = 2 \text{ }\mu\text{m}/\text{s}$  for active transport. We can see from Fig. 2.4 that the probability density function of the first hitting time for the passive transport has heavier tail behavior than the active transport. Due to the positive drift of the active transport, molecules will eventually arrive at the receiver. However, in the case of passive transport, molecules diffuse freely as Brownian motion, and some molecules might diffuse away and will not arrive at the receiver. The

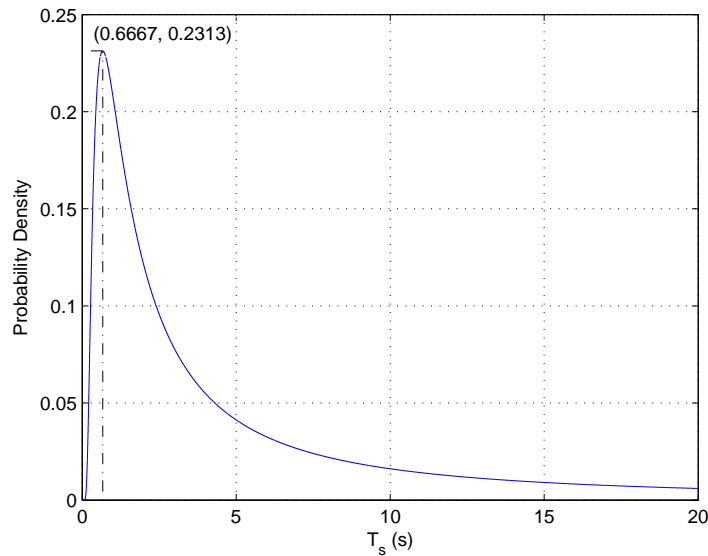


Figure 2.3: The PDF of the first hitting time for passive transport defined in (2.5) with  $D = 10^{-6} \text{ cm}^2/\text{s}$  and  $d = 20 \text{ }\mu\text{m}$ .

randomness (variance) of the first hitting time of the passive transport is much higher than the active transport.

## 2.2 Modulation of Diffusion-based Molecular Communication

In diffusion-based molecular communication, nanomachines can communicate with each other by modulating the information molecules in different ways, e.g., by concentration intensity, type of molecules, or by transmission time interval. Most of the molecular communication systems are assumed to be time-slotted, or *synchronous*, where the inter-transmission durations are fixed [35]. The information of synchronous systems is carried on either the level (amount or concentration intensity) [18, 32, 36] or the type [37, 38] of molecules. For example, in [39] isomers are used as messenger molecules to implement the synchronous type-based systems. In [40], *concentration shift keying* (CSK) and *molecule shift keying* (MoSK) are proposed, where CSK modulates the information through the variation in the concentration of the messenger molecules, and MoSK uses different types of messenger molecules to represent the information.

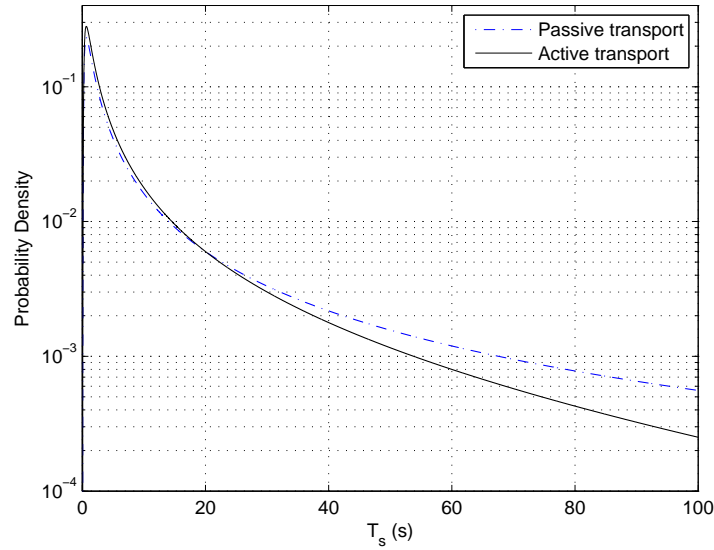


Figure 2.4: The PDF comparison of the first hitting time for active and passive transport defined in (2.2) and (2.5).

In *asynchronous* systems, where the inter-transmission durations are not restricted to be fixed, the information can be carried on the transmission time interval or the type of molecules as well. In [35], modulation factors are combined to embed additional information. The *mixed type – time* system utilizes the randomness of the inter-transmission times on the synchronous type-based system. These techniques can be used to increase the channel capacity and communication efficiency.

We consider the more commonly used synchronous communication systems in this thesis with the on-off keying (OOK) and the synchronous type-based modulation (TM) scenario. The OOK scenario is one of the synchronous level-based systems. The information bit ‘0’ is represented by remaining silent, while ‘1’ is represented by transmitting one molecule at the starting of each time-slot. In the case of TM, a transmitter encodes information by defining different types of molecules as different information, and it releases one molecule or remain silent at the starting of each time-slot as an information symbol. The details of how we implement the OOK and TM system are showed in Chapter 4 and 5, respectively.

## 2.3 Channel Characteristics

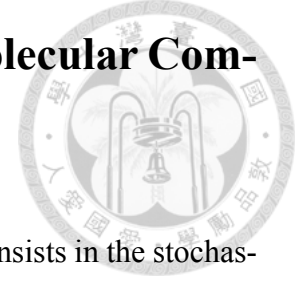


In diffusion-based molecular communication, since the molecules are drifting randomly, the arrival times of the molecules are hard to predict. The randomness effect causes the major obstacle for signal detection. Take the OOK system for example, when a 4-bit message  $(1, 0, 0, 0)$  is transmitted, one molecule is emitted at the beginning of the first symbol period, and then the transmitter remains silent for three symbol periods. If the molecule arrives in time during the first symbol period for detection, the receiver would detect the message correctly as  $(1, 0, 0, 0)$ . However, it is also possible that the molecule arrives late, which results in one of the four wrong decisions as:  $(0, 1, 0, 0)$ ,  $(0, 0, 1, 0)$ ,  $(0, 0, 0, 1)$ , or  $(0, 0, 0, 0)$ . We can see that the symbol ‘1’ crosses over with other symbol ‘0’s due to its late arrival. Depending on how late the molecule arrives, we can define different levels of crossover. We call it a *level- $j$  crossover* if the  $i$ -th transmitted molecule becomes the  $(i + j)$ -th to arrive [41].

In addition to the “crossover effect”, it is also possible for the receiver to pick up some molecules from the background environment and mistaken them as molecules sent by the transmitter. Consider the case of transmitting  $(0, 0, 0, 0)$  via OOK. No molecules are actually emitted, yet the receiver might still pick up some irrelevant molecules and claim to have received  $(0, 1, 0, 0)$ . This effect is the counterpart of the additive noise in traditional communications.

In a short summary, the physical channel in diffusion-based molecular communications is dominated by these two effects, the crossover and the additive noise. Depending on the environment, one behavior can be more dominant than the other. In conventional communication, noise is mainly considered as additional. It is the crossover effect that makes it hard to use the traditional channel coding concepts directly. Therefore, new channel coding distance functions need to be proposed for the molecular communication.

## 2.4 Channel Coding for Diffusion-based Molecular Communication



The randomness of diffusion-based molecular communication consists in the stochastic arrival times of the molecules [12]. In order to enhance reliability, we borrow the wisdom from the channel coding theory. The channel codes we consider in this thesis are fixed-length *block codes* with length  $m$  rather than other advanced channel coding schemes in order to fit the complexity constraint of the nanomachines. The notation  $[m, n]$  for block code is used to represent that each  $n$ -bit information is mapped to an  $m$ -bit codeword.

For illustration purpose, an example OOK system with  $[4, 2]$  block code applied is shown in Fig. 2.5(a), where the codebook is chosen to be

$$\{(0, 0, 0, 1), (0, 0, 1, 0), (0, 1, 1, 1), (1, 0, 1, 1)\}.$$

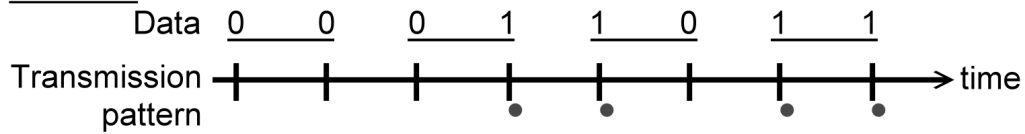
That is, the transmission pattern are  $(0, 0, 0, 1)$ ,  $(0, 0, 1, 0)$ ,  $(0, 1, 1, 1)$ , and  $(1, 0, 1, 1)$  when the data to be transmitted are ‘00’, ‘01’, ‘10’, and ‘11’, respectively. For example, if the data to be transmitted is ‘00011011’, then the coded data is ‘0001001001111011’.

In a TM system, a joint coding-modulation scheme is applied. The same coding rule described in the above example is first applied to the information data, and then different types of molecules are released according to the coded data. Molecule types  $A$ ,  $B$ , and  $C$  represent coded bits ‘01’, ‘10’, and ‘11’, respectively, and a silence represents ‘00’. For example, in Fig. 2.5(b), the transmission pattern for the data sequence ‘00011011’ is ‘0A0BACBC’, where ‘0’ means a silence at that time slot.

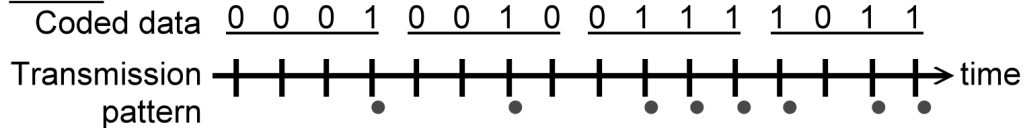


**On-off keying**

Uncoded



Coded

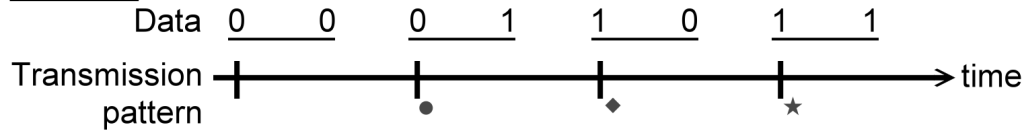


(a)

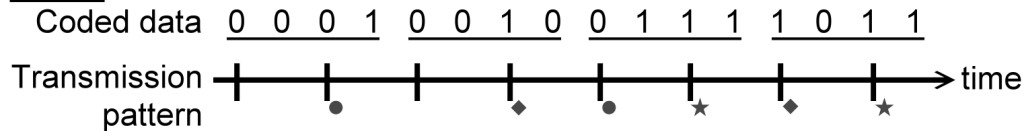
**Type-based**

Type A: ● Type B: ◆ Type C: ★

Uncoded



Coded



(b)

Figure 2.5: Coding scheme illustration for OOK and TM systems. A  $[4, 2]$  block code with codebook  $\{(0, 0, 0, 1), (0, 0, 1, 0), (0, 1, 1, 1), (1, 0, 1, 1)\}$  is used. In the OOK system, a molecule is released when the coded data bit is '1'. In the type-based modulation system, molecule types *A*, *B*, and *C* represent data bits '01', '10', and '11', respectively, and a silence represents '00'.





## Chapter 3

# Coding Distance Functions for Diffusion-based Molecular Communication

In most cases, the optimal decoding rule for a channel code is equivalent to the minimum distance (MD) rule with a proper definition of the distance between any two codewords. However, for molecular communication environments, existing distances may be unsuitable because the nature of molecular communication differs from the electromagnetic communication. In this chapter, we propose and discuss different categories of distance functions, which can help us measure the difference between codewords and further advance the channel coding application in diffusion-based molecular communication.

We first introduce the well-known Hamming distance, which has long been used in electromagnetic communication. We then define the notations and preliminaries for the following proposed distances, and give the optimal decoding distance function for a codeword pair. However, in practical molecular communication systems, codewords are transmitted one after another, i.e., serial transmission is employed. To obtain the optimal decoding distance function in the serial transmission scenario, we have to consider every combination of two transmitted sequences, and thus the complexity is extremely high. To tackle this problem, we propose two versions of distance functions that are applicable for



practical use.

The first one, called the *probability-based distance*, is a modified version of the optimal decoding distance by introducing a correcting term. The second distance function is the *pattern-based distance*, which calculates the distance by considering the codeword patterns only. The pattern-based distance has the advantage of lower computational complexity compared to the probability-based distance. Different from the distance functions in modern communication theory, distance functions we proposed for diffusion channels do not satisfy the symmetric property. Strictly speaking, a distance function (or a metric) in mathematics should satisfy the symmetric property. Nevertheless, in this thesis we still use the term distance function to comply with the tradition.

### 3.1 Hamming Distance

Hamming distance is defined as the number of bit differences between two codewords, and it is the most commonly used distance function in the study of conventional channel coding. In a binary symmetric channel, the MD decoding using Hamming distance is optimal if the codewords are transmitted with equal probability. The performance of a channel code is often indicated by the minimum Hamming distance among any codeword pairs in its codebook. Consequently, constructing a channel code with maximized minimum Hamming distance has long been considered as the channel coding design paradigm in traditional communications.

Nevertheless, in diffusion-based molecular communication, such paradigm may not work as well as in traditional communication due to the inherent properties of the Brownian motion channel. It is worth mentioning that the distance is no longer a symmetric function due to the crossover effect. In conventional communications, the channel is often assumed to be symmetric: the probability of sending 0 yet receiving 1 is the same as sending ‘1/ yet receiving ‘0’. Take the two codewords  $(0, 0, 0, 0)$  and  $(1, 0, 0, 0)$  for example. The symmetric channel results in  $\Pr\{(0, 0, 0, 0) \rightarrow (1, 0, 0, 0)\} = \Pr\{(1, 0, 0, 0) \rightarrow (0, 0, 0, 0)\}$ , and which leads to the symmetric nature of the Hamming distance, i.e.,  $d^{(H)}((0, 0, 0, 0), (1, 0, 0, 0)) = d^{(H)}((1, 0, 0, 0), (0, 0, 0, 0))$ , where the notation  $(0, 0, 0, 0)$

$\rightarrow (1, 0, 0, 0)$  refers to the event when  $(0, 0, 0, 0)$  is sent yet detected as  $(1, 0, 0, 0)$ .

However, in diffusion-based molecular communications, the symmetric channel property can no longer be assumed. When  $(0, 0, 0, 0)$  is transmitted, it can only be detected as  $(1, 0, 0, 0)$  if the receiver picks up molecule(s) from the background during the first symbol period. On the other hand, when  $(1, 0, 0, 0)$  is transmitted, the receiver would detect  $(0, 0, 0, 0)$  if the molecule emitted in the first symbol period arrives so late that it fails to arrive within four detection periods. In the scenario of molecular communication, the probabilities of these two events are assumed to be different, i.e.  $\Pr\{(0, 0, 0, 0) \rightarrow (1, 0, 0, 0)\} \neq \Pr\{(1, 0, 0, 0) \rightarrow (0, 0, 0, 0)\}$ . Thus, the commutative Hamming distance is no longer an optimal distance function for molecular communications. As a result, new distance functions should be proposed to achieve the optimal channel decoding for molecular communications.

## 3.2 Notations and Preliminaries

With the CDF given in (2.3) or (2.6), we can calculate the probability that a molecule does not arrive during the corresponding time slot, which is called the *crossover probability*. The probability that a molecule arrives during the corresponding time slot is

$$p_0 = F(T_c), \quad (3.1)$$

and the probability of arriving  $j \in \mathbb{N}$  time slot(s) late is

$$p_j = F((j+1)T_c) - F_{IG}(jT_c), \quad (3.2)$$

where  $F(t) = \int_0^t f(x)dx$  can be the cumulative distribution function of the inverse Gaussian distribution for active transport or the Lévy distribution for the passive transport, and  $T_c$  represents the duration of sending a coded bit. The term *level- $j$  crossover* is used to describe that a molecule is released by the transmitter in the  $i$ -th time slot but arrives at the receiver in the  $(i+j)$ -th time slot. The probability of having a level- $j$  crossover is

denoted by  $p_j$ .

Now consider the signal space of  $[m, n]$  block codes, which is denoted by

$$\mathcal{S} = \left\{ \mathbf{s} = (s_1, s_2, \dots, s_m) \mid s_i \in \{0, 1\}, i \in \{1, 2, \dots, m\} \right\}. \quad (3.3)$$

We define the addition and the scalar multiplication respectively as

$$\mathbf{x} + \mathbf{y} = (x_1 \oplus y_1, x_2 \oplus y_2, \dots, x_m \oplus y_m), \quad \forall \mathbf{x}, \mathbf{y} \in \mathcal{S}, \quad (3.4)$$

and

$$\beta \mathbf{x} = (\beta x_1, \beta x_2, \dots, \beta x_m), \quad \forall \mathbf{x} \in \mathcal{S}, \beta \in \{0, 1\}, \quad (3.5)$$

where the notation  $\oplus$  is defined as:  $0 \oplus 0 = 0$ ,  $0 \oplus 1 = 1$ ,  $1 \oplus 0 = 1$ , and  $1 \oplus 1 = 0$ .

In the signal space  $\mathcal{S}$ , all the codewords can be written as a linear combination of the standard basis, which comprises

$$\begin{aligned} \mathbf{e}_1 &= (1, 0, 0, \dots, 0), \quad \mathbf{e}_2 = (0, 1, 0, \dots, 0), \quad \dots, \\ \mathbf{e}_{m-1} &= (0, \dots, 0, 1, 0), \quad \mathbf{e}_m = (0, \dots, 0, 0, 1). \end{aligned} \quad (3.6)$$

Thus, given a codeword  $\mathbf{c} \in \mathcal{S}$ , it can be represented as

$$\mathbf{c} = (c_1, c_2, \dots, c_m) = c_1 \mathbf{e}_1 + c_2 \mathbf{e}_2 + \dots + c_m \mathbf{e}_m. \quad (3.7)$$

Note that for notational simplicity, we define  $\mathbf{e}_j = (0, 0, \dots, 0)$  for  $j > m$ . Due to the crossover effect of the diffusion channel, every element in  $\mathcal{S}$  may be right-shifted. The right-shift operator  $R_k : \mathcal{S} \rightarrow \mathcal{S}$  is defined by

$$R_k(\mathbf{e}_i) = \mathbf{e}_{i+k} \text{ for } k \in \mathbb{N} \cup \{0\}, \quad (3.8)$$

and the *shift pattern*  $\mathbf{k}$  is introduced to describe the crossover effect experienced by the codeword, where  $\mathbf{k} = (k_1, k_2, \dots, k_m)$  is a vector and  $k_i \in \mathbb{N} \cup \{0\}$  for  $1 \leq i \leq m$ . If

some codeword  $\mathbf{c}$  is shifted by  $\mathbf{k}$ , we denote the shifted codeword by  $R_{\mathbf{k}}(\mathbf{c})$ , which means that

$$R_{\mathbf{k}}(\mathbf{c}) = c_1 R_{k_1}(\mathbf{e}_1) + c_2 R_{k_2}(\mathbf{e}_2) + \dots + c_m R_{k_m}(\mathbf{e}_m). \quad (3.9)$$

Assuming that each bit in the codeword can be treated independently, i.e., each molecule diffuses independently, we can calculate the probability that  $\mathbf{c}$  experiences the shift pattern  $\mathbf{k}$ :

$$P(\mathbf{c}, \mathbf{k}) = \tilde{p}_1 \tilde{p}_2 \dots \tilde{p}_m, \quad (3.10)$$

where

$$\tilde{p}_i = \begin{cases} p_{k_i}, & \text{if } c_i = 1, \\ 1, & \text{if } c_i = 0, \end{cases} \quad i \in \{1, 2, \dots, m\}. \quad (3.11)$$

Note that when  $c_i = 0$ , it means that no molecules are released in the  $i$ -th time slot, and thus that probability needs not to be considered.

### 3.3 Optimal Distance Function for One-shot Transmission

By defining the distance function between two codewords  $\mathbf{x}$  and  $\mathbf{y}$  as

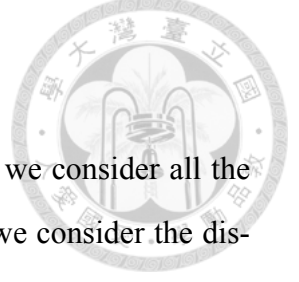
$$d(\mathbf{x}, \mathbf{y}) = -\log(\Pr\{\mathbf{x} \rightarrow \mathbf{y}\}), \quad (3.12)$$

where the notation  $\mathbf{x} \rightarrow \mathbf{y}$  represents the event that  $\mathbf{x}$  changes to  $\mathbf{y}$ , the optimal decoding distance function can be written as

$$d_{op}(\mathbf{x}, \mathbf{y}) = -\log \left\{ \sum_{\substack{\mathbf{k} \in \{\mathbb{N} \cup \{0\}\}^m, \\ k_i = 0 \text{ if } x_i = 0: R_{\mathbf{k}}(\mathbf{x}) = \mathbf{y}}} P(\mathbf{x}, \mathbf{k}) \right\}, \quad (3.13)$$

for all  $\mathbf{x}, \mathbf{y} \in \mathcal{S}$ . This distance calculates the summation of probabilities of all the possible transitions.

### 3.4 Probability-based Distance Function



For the case of serial transmission, the complexity is too high if we consider all the possibilities of transition patterns. Therefore, for practical reasons, we consider the distance function  $d_N(\mathbf{x}, \mathbf{y})$ , where the subscript  $N$  means that only crossover levels less than or equal to  $N$  are considered in calculating the crossover probabilities. This approximation is valid since high-level crossovers are less likely to happen. Given  $\mathbf{x}, \mathbf{y} \in S$ , the level- $N$  distance is defined to be

$$d_N(\mathbf{x}, \mathbf{y}) = -\log \left\{ \sum_{\substack{\mathbf{k} \in \{\mathbb{N} \cup \{0\}\}^m, k_i=0 \text{ if } x_i=0, \\ \|\mathbf{k}\|_\infty \leq N: R_{\mathbf{k}}(\mathbf{x})=\mathbf{y}}} P(\mathbf{x}, \mathbf{k}) \right\}. \quad (3.14)$$

where  $\|\mathbf{k}\|_\infty = \max_{1 \leq i \leq m} |k_i|$ . This distance calculates the summation of probabilities of the possible transitions with the crossover level smaller than or equal to  $N$ .

Now we consider the distance with the ISI correcting term. The notation  $E(\mathbf{y}, \mathbf{k})$  is used to denote the codeword obtained by replacing the 1's with 0's in the codeword  $\mathbf{y}$  according to the pattern  $\mathbf{k}$ : if the  $i$ -th element of  $\mathbf{k}$  is '1', the '1' at the corresponding position in  $\mathbf{y}$  should be replaced by a '0'. For example, if  $m = 4$ ,  $\mathbf{y} = (0, 1, 1, 1)$ , and  $\mathbf{k} = (0, 1, 0, 1)$ , then  $E(\mathbf{y}, \mathbf{k}) = (0, 0, 1, 0)$ . For any two  $\mathbf{x}, \mathbf{y} \in S$ , we define the probability-based distance  $d_{prob}(\mathbf{x}, \mathbf{y})$  as

$$d_{prob}(\mathbf{x}, \mathbf{y}) = -\log \left\{ \sum_{\mathbf{k} \in \{1,0\}^m} \mathbf{p}_{\text{ISI}}^{\mathbf{k}} (\mathbf{1} - \mathbf{p}_{\text{ISI}})^{(\mathbf{1}-\mathbf{k})} \times \exp[-d_N(\mathbf{x}, E(\mathbf{y}, \mathbf{k}))] \right\}, \quad (3.15)$$

where  $\mathbf{1}$  denotes the all-ones vector,  $\exp[-d_N(\mathbf{x}, E(\mathbf{y}, \mathbf{k}))]$  is the approximated probability of  $\mathbf{x}$  changing into  $E(\mathbf{y}, \mathbf{k})$  due to crossovers with level less than or equal to  $N$ , and the vector  $\mathbf{p}_{\text{ISI}}$ , called the *ISI correcting term*, is a constant vector that we can assign suitable values according to the diffusion environment. Here we use the multi-index to simplify the notation. For instance, if  $\mathbf{p}_{\text{ISI}} = (0.2, 0.1, 0.05, 0)$  and  $\mathbf{k} = (1, 1, 0, 0)$ , then  $\mathbf{p}_{\text{ISI}}^{\mathbf{k}} = 0.2^1 \times 0.1^1$ . The probability-based distance (3.15) calculates the summation of probabilities of

the possible transitions with the crossover level smaller than or equal to  $N$ , considering the inter-symbol crossover effect and the background noise with the help of the ISI correcting term.

In this thesis, we set the  $\mathbf{p}_{\text{ISI}}$  to be  $(p_{\text{noise}} + \frac{1}{2}p_1, p_{\text{noise}} + \frac{1}{2}p_2, p_{\text{noise}} + \frac{1}{2}p_3, p_{\text{noise}} + \frac{1}{2}p_4)$ , where  $p_{\text{noise}}$  is the probability of having an background noise in each time slot, and  $p_j$  is the probability of having a level- $j$  crossover. We assume that the ISI noise molecule is from the last bit of the previous symbol. The reason why we simplify the ISI noise as originating from the last bit of the previous symbol is because the probability of having lower level crossover is much higher. Therefore, if we have an ISI noise in the first time slot in the current symbol, we regard the ISI noise molecule as the last bit of the previous symbol having a level-1 crossover with probability  $p_1$ . Similarly, the ISI noise molecule arriving at the second, third and fourth time slot in the current symbol is considered as the last bit of the previous symbol having level-2, level-3 and level-4 crossover with probability  $p_2$ ,  $p_3$ , and  $p_4$ , respectively. The ' $\frac{1}{2}$ ' term comes from assuming the probability of the last bit of the previous symbol equals 1 is  $\frac{1}{2}$ .

### 3.5 Pattern-based Distance Function

In this section we propose the pattern-based decoding distance, in which the distance value depends only on the bit pattern transitions. The concept of the pattern-based distance is about simplifying the calculation from multiplying probabilities as the probability-based distance to the summation of crossover levels in the transmission of a symbol. To obtain the pattern-based distance value  $d_{\text{patt}}(\mathbf{x}, \mathbf{y})$  from codeword  $\mathbf{x}$  to codeword  $\mathbf{y}$ , we first subtract  $\mathbf{y}$  from  $\mathbf{x}$ , and call the subtraction result **diff**. Since the codewords  $\mathbf{x}$  and  $\mathbf{y}$  both belong to  $\mathcal{S}$  and the bits of  $\mathbf{x}$  and  $\mathbf{y}$  belong to  $\{0, 1\}$ , each entry of **diff** only has three possible values: '0', '1' and '-1'. If an entry of **diff** is '0', it means that the corresponding entries of  $\mathbf{x}$  and  $\mathbf{y}$  are both zero or both one; if '1' appears in an entry of **diff**, it means that the molecule expected to arrive in that corresponding time slot arrives in a later time slot; if a '-1' appears in an entry of **diff**, it means that the receiver captures irrelevant molecules in this time slot.

With the help of **diff**, we can compute the distance by the following process. For each ‘1’ in **diff**, we find the first ‘1’ in **y** appearing *after* this entry and calculate the delay in terms of the number of entries; meanwhile, we eliminate the ‘-1’ in **diff** in the same entry as the ‘1’ in **y** that we just found. If there is no ‘1’ in **y** after this entry, we simply assume the corresponding molecule to arrive in the first time slot of the next symbol duration. For those -1’s that are not eliminated, we assume that the redundant molecules come from the last bit of the previous symbol. Those delays are also calculated in terms of the number of entries. Then, the total delay is defined to be the pattern-based distance from **x** to **y**, and is denoted by  $d_{patt}(\mathbf{x}, \mathbf{y})$ . This value represents an approximate total number of time slot delays in the transmission of a symbol, and thus is suitable for a distance measure between codewords.

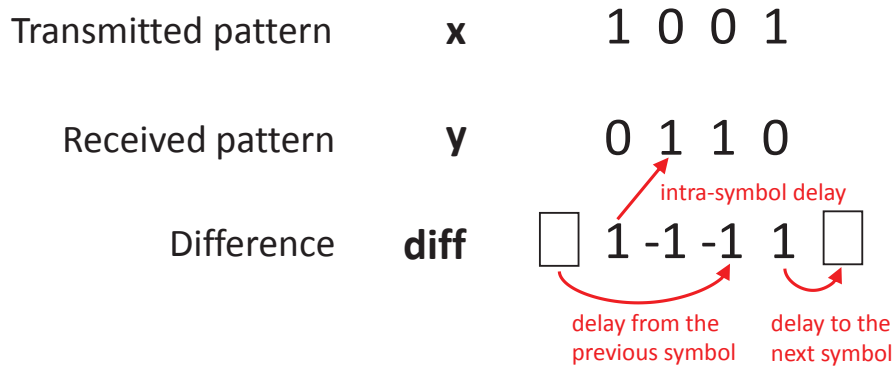


Figure 3.1: Example of calculating the pattern-based distance.

Fig. 3.1 is an example for calculating the pattern-based distance with  $\mathbf{x} = (1, 0, 0, 1)$  and  $\mathbf{y} = (0, 1, 1, 0)$ . The subtraction result **diff** in the example is  $(1, -1, -1, 1)$ . The ‘1’ in the first entry of **diff** corresponds to the ‘1’ in the second entry of **y**, showing one time slot delay. The ‘-1’ in the second entry of **diff** is then eliminated. The ‘1’ in the fourth entry of **diff** has no corresponding ‘1’ in **y**, and thus we assume it to arrive in the first time slot of the next symbol duration, having a single time slot delay. Since the ‘-1’ at the third entry of **diff** is not eliminated, we regard this as having an interfering molecule from the last bit of the previous symbol with a delay of three time slots. From the above discussions, we can calculate  $d_{patt}(\mathbf{x}, \mathbf{y})$  as  $1 + 1 + 3 = 5$ . Algorithm 1 summarizes the calculation of the pattern-based decoding distance  $d_{patt}(\mathbf{x}, \mathbf{y})$ .



---

**Algorithm 1** Calculation of the pattern-based distance from codeword  $\mathbf{x}$  to codeword  $\mathbf{y}$  for an  $(m, n)$  block code.

---

**Initialization:**  $d_{patt}(\mathbf{x}, \mathbf{y}) \leftarrow 0$

**Output:**  $d_{patt}(\mathbf{x}, \mathbf{y})$

```
1: for  $i = 1$  to  $m$  do
2:   diff[ $i$ ]  $\leftarrow \mathbf{x}[i] - \mathbf{y}[i]$ 
3: end for
4: for  $i = 1$  to  $m$  do
5:   if diff[ $i$ ] = 1 then
6:     if there is any 1 in  $\mathbf{y}$  after index  $i$  then
7:        $j \leftarrow$  the index of the nearest 1
8:        $d_{patt}(\mathbf{x}, \mathbf{y}) \leftarrow d_{patt}(\mathbf{x}, \mathbf{y}) + (j - i)$ 
9:       diff[ $j$ ]  $\leftarrow 0$ 
10:    else
11:       $d_{patt}(\mathbf{x}, \mathbf{y}) \leftarrow d_{patt}(\mathbf{x}, \mathbf{y}) + (m + 1 - i)$ 
12:    end if
13:  end if
14: end for
15: for  $i = 1$  to  $m$  do
16:   if diff[ $i$ ] = -1 then
17:      $d_{patt}(\mathbf{x}, \mathbf{y}) \leftarrow d_{patt}(\mathbf{x}, \mathbf{y}) + i$ 
18:   end if
19: end for
```

---







## Chapter 4

# Channel Coding Design for On-off

## Keying Modulation

In this chapter, we propose the channel coding design for on-off keying (OOK) modulation. We first introduce the OOK modulation, and then use minimum distance (MD) decoding rule to implement decoding. We compare the symbol error rate (SER) performance using MD decoding with distance functions: probability-based distance, pattern-based distance and Hamming distance. The numerical results show that our proposed distances decoding rules are near-optimal, and Hamming distance may not be suitable especially for the cases of active transport.

### 4.1 On-off Keying Modulation

As shown in Fig. 4.1, OOK is a modulation scheme in which the transmitter conveys a single molecule to represent information bit '1' while the transmitter remains silent to represent information bit '0'. We adopt the hard-decision decoding for the OOK system. That is, if no molecule arrives in the corresponding time slot, the information bit is detected as '0'; when there are greater than or equal to one molecule, the information bit is detected as '1'.

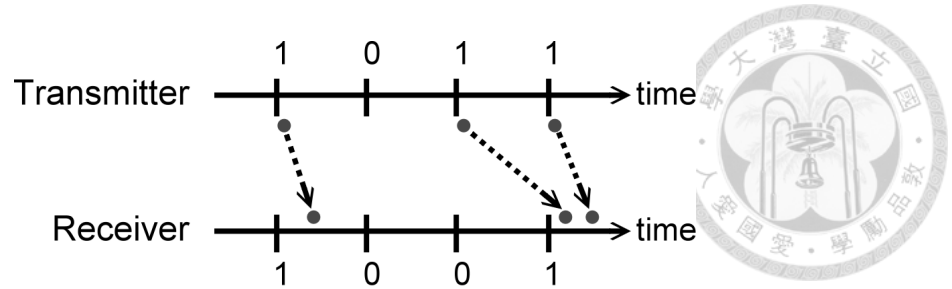


Figure 4.1: Illustration of the on-off keying (OOK) modulation scheme.

## 4.2 Minimum Distance Decoding for On-off Keying Modulation

The minimum distance (MD) decoding rule for OOK systems works as follows. First the signal space  $\mathcal{S}$  is partitioned into  $2^n$  decoding regions  $D^{(1)}, D^{(2)}, \dots, D^{(2^n)}$ , and  $\mathcal{S} = \bigcup_{k \in \{1, \dots, 2^n\}} D^{(k)}$ . The distance from a signal pattern to each codeword is calculated. If this signal pattern has minimum distance to codeword  $k$ , where  $1 \leq k \leq 2^n$ , then this signal pattern belongs to decoding region  $k$ . That is, whenever the receiver acquires a signal that belongs to region  $k$ , this signal is decoded as codeword  $k$ .

## 4.3 Numerical Results

In this section we numerically compare the symbol error rate (SER) results of the coded and uncoded scenarios under different decoding criteria for OOK scenario of both active and passive transport systems. The simulation environment is based on the calcium signaling [32] by setting the diffusion coefficient  $D = 10^{-6} \text{ cm}^2/\text{s}$ , the distance between the transmitter and the receiver  $d = 20 \text{ }\mu\text{m}$ , and the drift velocity  $v = 2 \text{ }\mu\text{m/s}$  in active transport. The channel codes used for simulations are  $[4, 2]$  block codes, which means that there are  $\binom{2^4}{4} = 1820$  possible codebook selections and there are  $4^{16}$  decoding rules for each codebook selection. When calculating the probability-based distance, we use  $N = 4$ . In order to compare the uncoded and coded scenario fairly, we use the same average bit duration  $T$ , which is the average period to send one information bit.

### 4.3.1 Active Transport via Brownian Motion with Drift

In Fig. 4.2, we show the SER distribution over all codebooks under different decoding rules for OOK systems when  $T = 100$  s. We show the results using the decoding rules by Hamming distance, probability-based distance, pattern-based distance, and the optimal decoding rule. The decoding rule that results in the lowest SER through exhaustive search are chosen to generate the curves of optimal decoding rule, which serves as the lower bound for the SER. The codebooks are indexed by the order of descending SER using the optimal decoding rule for figure clarity. We can see that most of the codebooks do not lead to better performance than the uncoded system, and in fact, there are only 29 codebooks that result in better performance than the uncoded system when using the optimal decoding. None of the cases decoding with the Hamming distance has SER performance better than the uncoded scenario. There are 28 and 18 codebooks perform better than the uncoded scenario when using the MD decoding with the probability-based distance and the pattern-based distance, respectively. As a result, choosing a suitable codebook is critical designing the channel coding of diffusion-based molecular communication system.

The SER of the uncoded scenario is 1.57%. The best SERs are 1.04% using the optimal decoding rule, 1.04% using the MD decoding with the probability-based distance, 1.05% using the MD decoding with the pattern-based distance, and 2.44% using the MD decoding with the Hamming distance, respectively. It is worth noting that we can see from Fig. 4.2 the SERs decoding with the probability-based distance approaches the case using the optimal decoding rule that the SER curve is almost overlapped.

We show the best performance codebook with the optimal decoding rule and the corresponding decoding regions under different decoding criteria for  $T = 100$  s. The best performance codebook is:

$$\{(0, 0, 0, 0), (0, 0, 1, 0), (1, 0, 0, 0), (1, 1, 1, 0)\}.$$

We observed that the last bit of the above four code words are all zero, which can reduce crossovers between symbols, and thus lowers the inter-symbol interference (ISI) and

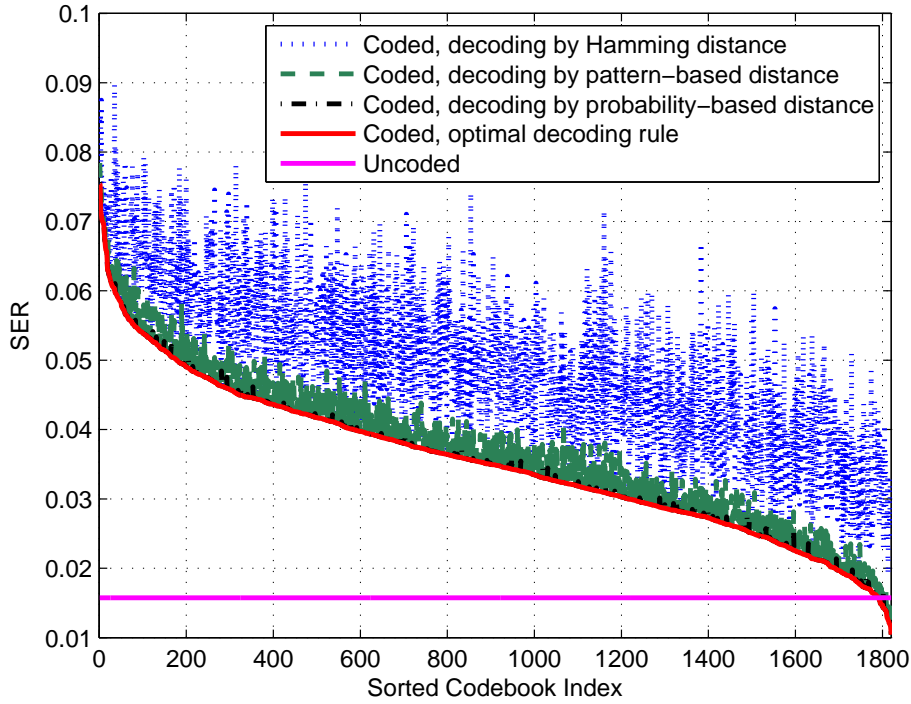


Figure 4.2: SER distribution under different decoding rules for OOK systems with  $T = 100$  s. The codebooks are indexed by the order of descending SER using the optimal decoding rule.

SER. The decoding rule using the probability-based distance is exactly the same as the optimal one, and the rule is shown in Table 4.1. There is only one codeword decoding with the pattern-based distance being decoded differently from the optimal decoding rule:  $(1, 0, 0, 1)$  decoded into  $\mathbf{c}^{(2)}$  rather than  $\mathbf{c}^{(3)}$  as the optimal decoding rule. The decoding region using the Hamming distance has three codewords being decoded differently from the optimal decoding rule:  $(0, 0, 0, 1)$  decoded into  $\mathbf{c}^{(1)}$  rather than  $\mathbf{c}^{(2)}$ ,  $(0, 1, 0, 0)$  decoded into  $\mathbf{c}^{(1)}$  rather than  $\mathbf{c}^{(3)}$ , and  $(0, 1, 0, 1)$  decoded into  $\mathbf{c}^{(1)}$  rather than  $\mathbf{c}^{(4)}$ .

Fig. 4.3 shows the SERs under various  $T$  using different decoding criteria. For each decoding rule, the best codebook, which is the codebook with the lowest SER, for that average bit duration  $T$  is adopted. It is shown that channel coding effectively lowers the SER for OOK systems, as long as a proper decoding method is adopted. The Hamming distance decoding is apparently non-applicable, especially when  $T$  is large. It can be seen that the performance of the MD decoding using either the probability-based distance or the pattern-based distance is very close to that using the optimal decoding rule, showing



Table 4.1: The best performance codebook and the corresponding decoding regions under the optimal decoding rule and the probability-based distance.

Codeword	$\mathbf{c}^{(1)} = (0, 0, 0, 0)$	$\mathbf{c}^{(2)} = (0, 0, 1, 0)$
Decoding Region	$(0, 0, 0, 0)$	$(0, 0, 0, 1)$ $(0, 0, 1, 0)$ $(0, 0, 1, 1)$
Codeword	$\mathbf{c}^{(3)} = (1, 0, 0, 0)$	$\mathbf{c}^{(4)} = (1, 1, 1, 0)$
Decoding Region	$(0, 1, 0, 0)$ $(1, 0, 0, 0)$ $(1, 0, 0, 1)$	$(0, 1, 0, 1)$ $(0, 1, 1, 0)$ $(0, 1, 1, 1)$ $(1, 0, 1, 0)$ $(1, 0, 1, 1)$ $(1, 1, 0, 0)$ $(1, 1, 0, 1)$ $(1, 1, 1, 0)$ $(1, 1, 1, 1)$

the effectiveness of the proposed distances.

To discuss thoroughly about the probability-based distance, the pattern-based distance, and the Hamming distance, we compare their performances with the optimal decoding rule under different  $T$ . In Fig. 4.4, we show the amount of codebooks decoding by MD with the probability-based, the pattern-based, and the Hamming distance having the same performance as the optimal decoding rule. We can see that much more codebooks have the same performance as the optimal decoding in the case of decoding by probability-based distance. There are more than 1000 codebooks decoding with the probability-based distance having the same performance as the optimal decoding rule, except the case with  $T = 20$  s, where the SER is higher than 25% and the time slot is not long enough for good communication. The cases of decoding with the Hamming distance are much worse and not suitable for decoding in active transport, and there are only about 30 codebooks performing exactly as the optimal decoding rule.

As shown in Fig. 4.5, we compare the performance between the probability-based, the pattern-based, and the Hamming distance, and show the amount of codebook for each distance having the best SER performance among the three distances. We can see that the probability-based distance outperforms other distances with having more than 1400 codebooks performing the best among all cases of  $T$ . The pattern-based distance has the

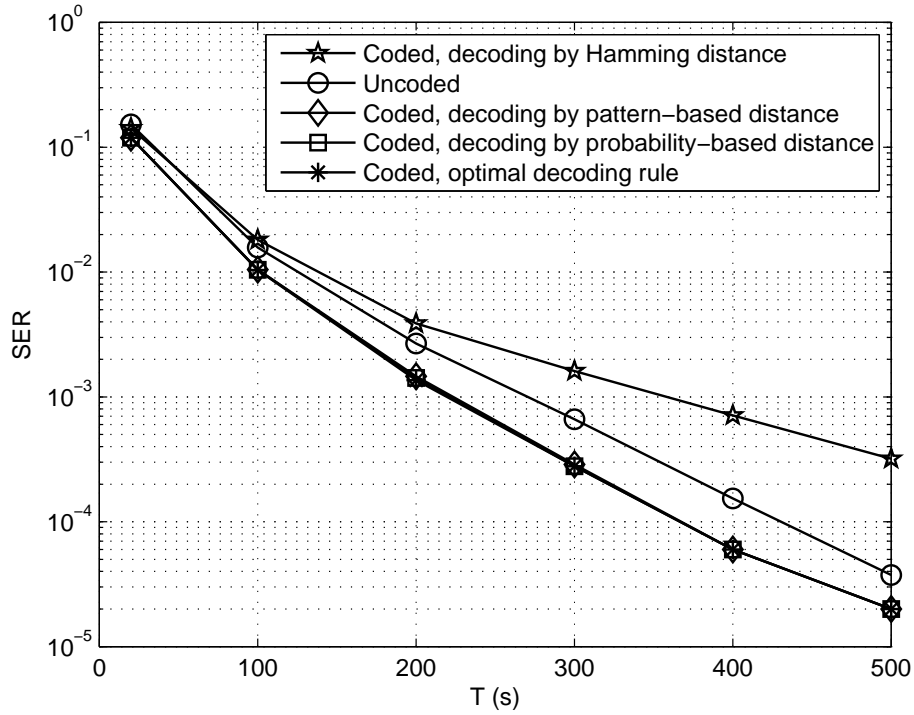


Figure 4.3: Comparison of SER performances for the uncoded OOK system and the coded OOK systems employing optimal decoding rule, MD decoding with probability-based distance, MD decoding with pattern-based distance, and MD decoding with Hamming distance.

best SER performance for 400 to 1200 codebooks under different  $T$ . Except the case with  $T = 20$  s, the performance of the pattern-based distance is better when  $T$  is larger. The Hamming distance has only about 60 codebooks having the lowest SER. Combining with the observation results in Fig. 4.2, Fig. 4.3, and Fig. 4.4, we can conclude that the Hamming distance is unsuitable for the active transport for diffusion-based molecular communication. Another conclusion is that the probability-based distance leads to better results in most practical cases. However, the pattern-based distance has the advantage of lower computational complexity; therefore, choosing the probability-based distance or the pattern-based distance can be considered a tradeoff between SER performance and computational complexity.

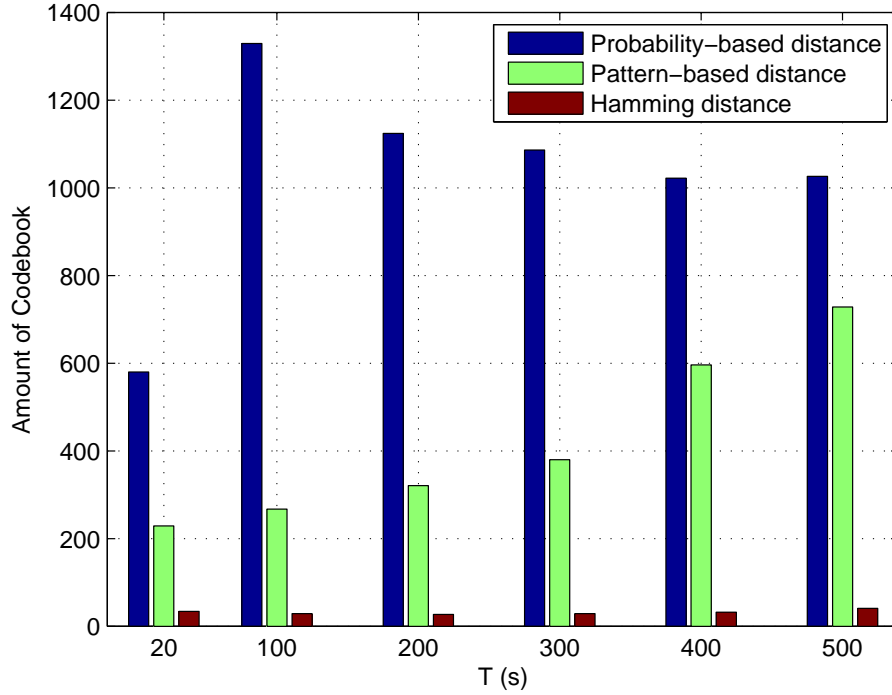


Figure 4.4: The amount of codebooks decoding by MD with the probability-based, the pattern-based, and the Hamming distance having the same performance as the optimal decoding rule under different  $T$  for OOK systems.

### 4.3.2 Passive Transport via Brownian Motion

We give parallel numerical results for the passive transport as the active transport. In Fig. 4.6, we show the SER distribution over all codebooks under the Hamming distance, probability-based distance, pattern-based distance, and the optimal decoding rule for OOK systems when  $T = 100$  s. The optimal decoding rule is generated through searching the lowest SER exhaustively. The codebooks are indexed by the order of descending SER using the optimal decoding rule for figure clarity. We see that adopting channel coding can indeed improve the SER result than the uncoded system, and there are 418 codebooks that result in better performance than the uncoded system using the optimal decoding rule, which is much more than the case of with drift (29 codebooks.) For the cases of decoding with the Hamming distance, the probability-based distance, and the pattern-based distance, there are 225, 340, and 157 codebooks performing better than the uncoded scenario respectively.

The best SERs are 10.94% using the optimal decoding rule, 10.94% using the MD de-



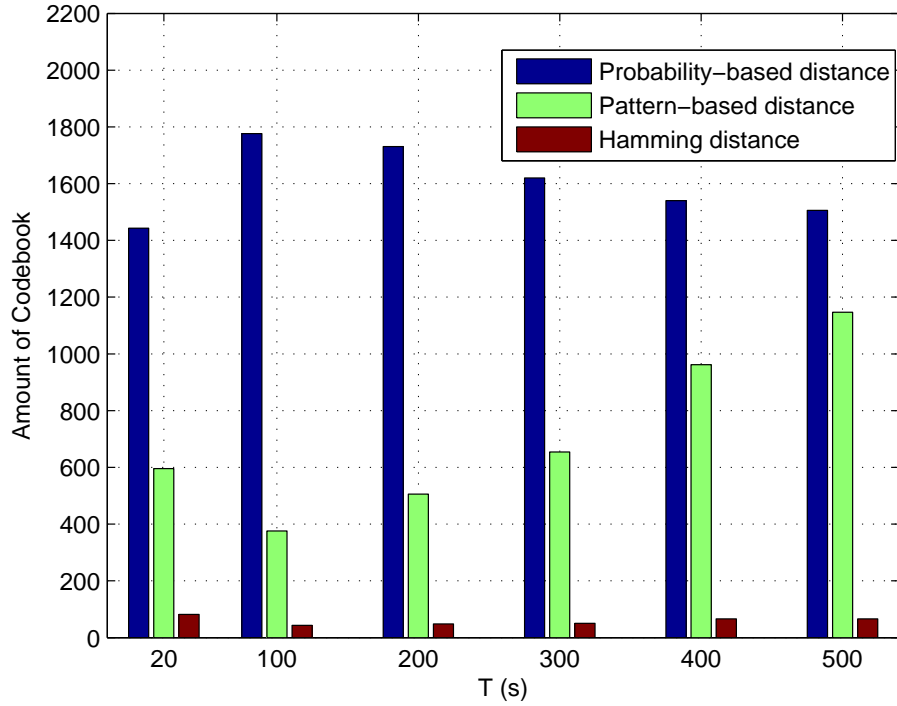


Figure 4.5: The amount of codebook performing the best among MD decoding with the probability-based, the pattern-based, and the Hamming distance under different  $T$  for OOK systems.

coding with the Hamming distance, 11.44% using the MD decoding with the probability-based distance, and 11.83% using the MD decoding with the pattern-based distance, respectively; while the SER is 14.72% for the uncoded scenario. The performance of the results decoding with the Hamming distance in active transport is much worse than the uncoded scenario and both the probability-based distance and the pattern-based distance. However, in passive transport, the Hamming distance performs better than the uncoded scenario in some (225) codebooks.

We show the best performance codebook with the optimal decoding rule in Table 4.2 for  $T = 100$  s. The best performance codebook codebook is:

$$\{(0, 0, 0, 0), (0, 0, 1, 1), (0, 1, 0, 0), (1, 1, 1, 0)\}.$$

The decoding rule using the Hamming distance has one codebook being decoded differently from the optimal decoding rule:  $(0, 1, 1, 1)$  decoded into  $\mathbf{c}^{(2)}$  rather than  $\mathbf{c}^{(4)}$ . The

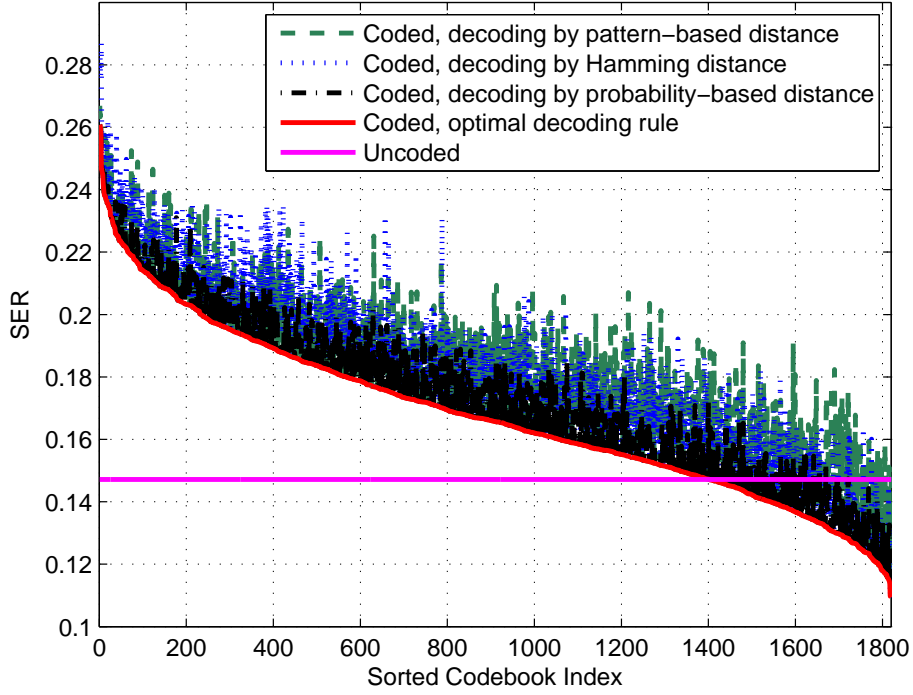
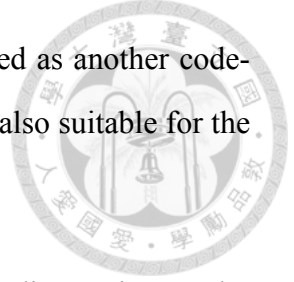


Figure 4.6: SER distribution under different decoding rules for OOK systems with  $T = 100$  s. The codebooks are indexed by the order of descending SER using the optimal decoding rule.

decoding rule using the probability-based distance has two codebooks being decoded differently from the optimal decoding rule:  $(0, 1, 1, 1)$  and  $(1, 0, 1, 1)$  are decoded into  $\mathbf{c}^{(4)}$  rather than  $\mathbf{c}^{(2)}$ . The decoding rule using the pattern-based distance has five codebooks being decoded differently from the optimal decoding rule:  $(0, 0, 1, 0)$  decoded into  $\mathbf{c}^{(3)}$  rather than  $\mathbf{c}^{(2)}$ ,  $(0, 1, 0, 1)$  decoded into  $\mathbf{c}^{(4)}$  rather than  $\mathbf{c}^{(3)}$ ,  $(1, 0, 0, 1)$  decoded into  $\mathbf{c}^{(1)}$  rather than  $\mathbf{c}^{(4)}$ ,  $(1, 1, 0, 0)$  decoded into  $\mathbf{c}^{(3)}$  rather than  $\mathbf{c}^{(4)}$ , and  $(1, 1, 1, 1)$  decoded into  $\mathbf{c}^{(2)}$  rather than  $\mathbf{c}^{(4)}$ .

We can see that the pattern-based distance might not be suitable for the passive transport, because the concept of the pattern-based distance is to focus on the bit pattern transitions caused by the asymmetric crossover effect. However, in the scenario of the passive transport, the molecules diffuse freely as Brownian random walk, which is more like a symmetric process. On the contrary, the symmetry of the Hamming distance happens to make the Hamming distance a suitable distance for the passive transport. Although the probability-based distance is also asymmetric, but the probability-based distance calcu-



lates the probability approximation of one codeword sent yet detected as another codeword. Thus, the probability-based distance still performs well and is also suitable for the passive transport.

Table 4.2: The best performance codebook and the corresponding decoding regions under the optimal decoding rule.

Codeword	$\mathbf{c}^{(1)} = (0, 0, 0, 0)$	$\mathbf{c}^{(2)} = (0, 0, 1, 1)$
Decoding Region	(0, 0, 0, 0) (1, 0, 0, 0)	(0, 0, 0, 1) (0, 0, 1, 0) (0, 0, 1, 1) (0, 1, 1, 1) (1, 0, 1, 1)
Codeword	$\mathbf{c}^{(3)} = (0, 1, 0, 0)$	$\mathbf{c}^{(4)} = (1, 1, 1, 0)$
Decoding Region	(0, 1, 0, 0) (0, 1, 0, 1)	(0, 1, 1, 0) (1, 0, 0, 1) (1, 0, 1, 0) (1, 1, 0, 0) (1, 1, 0, 1) (1, 1, 1, 0) (1, 1, 1, 1)

Fig. 4.7 shows the SERs under various  $T$  using different decoding criteria. For each decoding rule, the best codebook for that bit duration  $T$  is adopted. We can see that channel coding indeed effectively lowers the SER for OOK systems in passive transport as well. The performance of the MD decoding using the Hamming distance and the probability-based distance is similar to the optimal decoding rule, and the performance of the coded of pattern-based distance is slightly higher but is still better than the uncoded scenario.

Again, to discuss thoroughly about the probability-based distance, the pattern-based distance, and the Hamming distance, we compare their performances with the optimal decoding rule under different bit duration  $T$ . In Fig. 4.8, we show the number of codebooks decoding by MD with the probability-based, the pattern-based, and the Hamming distance performing the same as the optimal decoding rule. We can see that much more codebooks have the same performance as the optimal decoding in the case of decoding by probability-based distance, there are about 400 codebooks except the case with  $T = 20$  s, where the SER is higher than 25%, and the time slot is not long enough for good communication. Although Fig. 4.7 shows that the SER of the best codebook with MD decoded by the

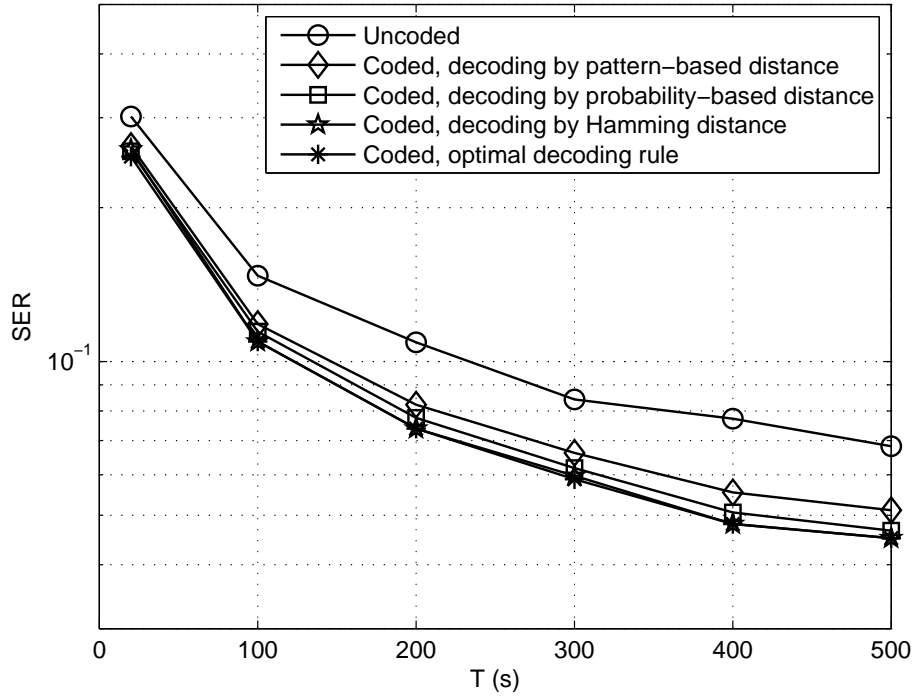


Figure 4.7: Comparison of SER performances for the uncoded OOK system and the coded OOK systems employing optimal decoding rule, MD decoding with probability-based distance, MD decoding with pattern-based distance, and MD decoding with Hamming distance.

Hamming distance is better than the case of the probability-based distance, in Fig. 4.8 we can see that more codebooks decoded by the probability-based distance have the same SER performance as the optimal decoding rule than the Hamming distance.

As shown in Fig. 4.9, we compare the performance between the probability-based, the pattern-based, and the Hamming distance, and show the amount of codebook for each distance having the best SER performance among the three distances. We can see that the probability-based distance outperforms other distances with having more than 1200 codebooks performing the best among all cases of  $T$ . The pattern-based distance and the Hamming distance have similar performance, both performing the best for about 400 codebooks. We conclude that the probability-based distance leads to better results in most practical cases. Note that, however, the pattern-based distance and the Hamming distance have the advantage of low computational complexity. Therefore, choosing the probability-based distance, the pattern-based distance, or the Hamming distance can be considered a tradeoff between SER performance and computational complexity.

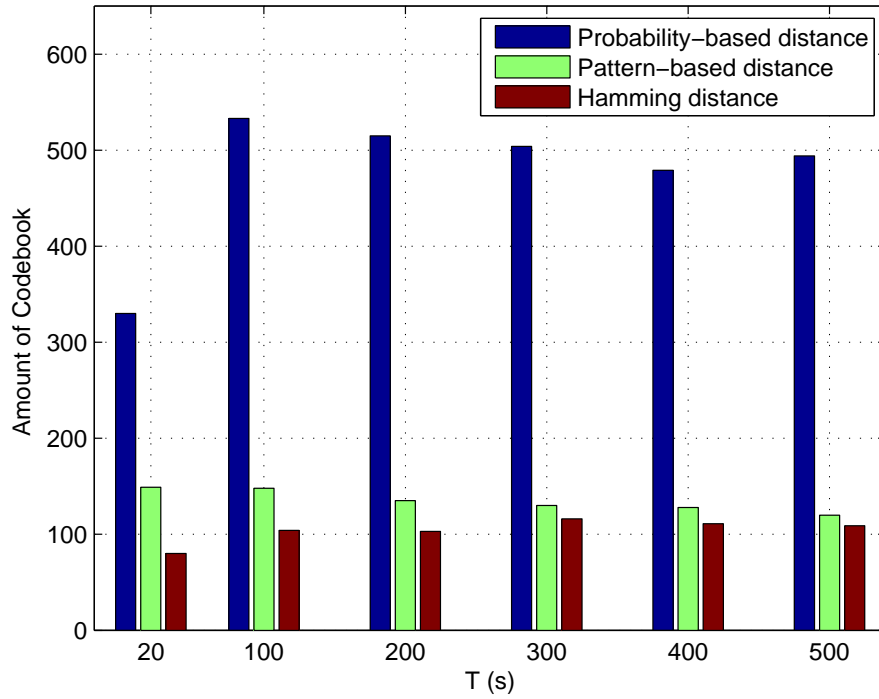


Figure 4.8: The amount of codebooks decoding by MD with the probability-based, the pattern-based, and the Hamming distance having the same performance as the optimal decoding rule under different  $T$  for OOK systems.

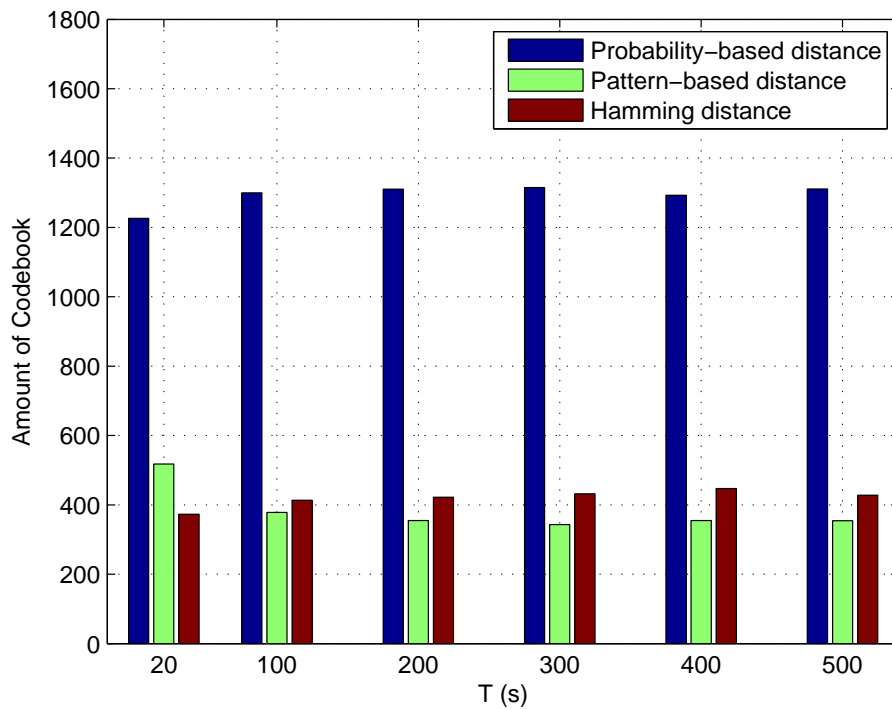


Figure 4.9: The amount of codebook performing the best among MD decoding with the probability-based, the pattern-based, and the Hamming distance under different  $T$  for OOK systems.



## Chapter 5

# Channel Coding Design for Synchronous Type-based Modulation

In this chapter, we demonstrate how the channel coding concept can be applied for type-based modulation (TM) system. After introducing the TM system, the minimum distance (MD) decoding rule to implement decoding for TM is proposed. The numerical results are presented with the uncoded and coded scenarios under different MD decoding functions. Similar to the results in OOK system, the symbol error rate (SER) performance of our proposed distances decoding rules are near-optimal, and Hamming distance may not be suitable especially for the cases of active transport.

### 5.1 Synchronous Type-Based Modulation

In a synchronous type-based modulation (TM) system, the transmitter sends messages by releasing a sequence of molecules of different types. Each molecule belongs to a type of molecules in the *type set*  $Q$  and each type represents a certain information [42]. Take  $Q = \{A, B, C\}$  for instance, there are three types of molecules: type- $A$ , type- $B$ , and type- $C$ . If the information bits are grouped two by two, information can be delivered in the following way: if the data bits are '00', the transmitter remains silent, while if the data bits are '01', '10', and '11', the transmitter releases molecules of type  $A$ ,  $B$ , and  $C$ , respectively. Note that we assume that the receiver can perfectly recognize the molecule

type once the molecule is caught.



## 5.2 Minimum Distance Decoding for Synchronous Type-based Modulation

Other than OOK systems, the MD decoding using the proposed distance functions is also applicable to TM systems with minor modifications. Under the assumption that the receiver can distinguish different types of molecules perfectly once they are caught, a TM system can be regarded as a superposition of *multiple OOK sub-systems that operate independently* with each sub-system consisting of only a single type of molecules. With this, we propose to calculate the distance values of this “compound system” based on the distance values of the OOK sub-systems. Suppose that there are  $M$  types of molecules in a type-based modulation system, and we want to define the distance value between the codeword  $\mathbf{x}$  and the received *pattern*  $\hat{\mathbf{y}}$  (Notice that  $\hat{\mathbf{y}}$  is a compound pattern, not a codeword.) By transforming the codeword  $\mathbf{x}$  into  $\mathbf{x}_1, \dots, \mathbf{x}_M$ , with  $\mathbf{x}_i$  being the transmission pattern corresponding to type- $i$  molecules, and decomposing  $\hat{\mathbf{y}}$  into  $\mathbf{y}_1, \dots, \mathbf{y}_M$  with  $\mathbf{y}_i$  being a codeword in the OOK sub-system corresponding to type- $i$  molecules, the distance between  $\mathbf{x}$  and  $\hat{\mathbf{y}}$  for the compound system is given by

$$d_{comp}(\mathbf{x}, \hat{\mathbf{y}}) = \sum_{i=1}^M c_i d(\mathbf{x}_i, \mathbf{y}_i), \quad (5.1)$$

where  $d$  is the distance function (either Hamming, probability-based or pattern-based) of the sub-system and  $c_i$  is the weighting for type- $i$  molecules and  $\sum_{i=1}^M c_i = 1$ . The weighting  $c_i$  can be chosen according to the diffusion properties of each molecule due to, for example, different radius and different diffusion coefficients. In case that the molecules have similar diffusion behaviors, we can assign equal coefficients  $c_i = 1/M, i = 1, 2, \dots, M$  for simplicity.

We use Fig. 5.1 to demonstrate the minimum distance decoding process for the type-based modulation systems. Assume that there are three different types of molecules  $A, B,$

Data	0 0	0 1
Coded data	0 0 0 1	0 0 1 0
Transmission patterns of each OOK sub-system	Type A	Type A
	Type B	Type B
	Type C	Type C
Data	1 0	1 1
Coded data	0 1 1 1	1 0 1 1
Transmission patterns of each OOK sub-system	Type A	Type A
	Type B	Type B
	Type C	Type C

Figure 5.1: Demonstration of the minimum distance decoding process for the type-based modulation systems. The TM system is decomposed into three OOK sub-systems. Molecule types *A*, *B*, and *C* represent data bits ‘01’, ‘10’, and ‘11’, respectively, and a silence represents ‘00’. We use the  $[4, 2]$  block code with codebook  $\{(0, 0, 0, 1), (0, 0, 1, 0), (0, 1, 1, 1), (1, 0, 1, 1)\}$  for example.

and *C*. We use the  $[4, 2]$  block code with codebook  $\{(0, 0, 0, 1), (0, 0, 1, 0), (0, 1, 1, 1), (1, 0, 1, 1)\}$ . If the data bits are ‘00’, for instance, the coded pattern is ‘(0, 0, 0, 1)’, the transmitting pattern will be ‘01’ for type-*A* molecules and ‘00’ for both type-*B* and type-*C* molecules. Equal coefficients  $c_i = \frac{1}{3}$  are chosen, and the pattern-based distance is used for demonstration. During decoding, if the receiver detects ‘01’ for type-*A*, ‘00’ for type-*B*, and ‘10’ for type-*C* molecules, the distance between the codeword (0, 0, 0, 1) and the detected results is calculated as  $\frac{1}{3}\{d_{patt}((0, 1), (0, 1)) + d_{patt}((0, 0), (0, 0)) + d_{patt}((0, 0), (1, 0))\} = \frac{1}{3}(0 + 0 + 1) = \frac{1}{3}$ . Similarly, the distance is  $\frac{1}{3}(2 + 1 + 1) = \frac{4}{3}$  between the codeword (0, 0, 1, 0) and the detected results,  $\frac{1}{3}(1 + 0 + 2) = 1$  between the codeword (0, 1, 1, 1) and the detected results, and  $\frac{1}{3}(2 + 2 + 2) = 2$  between the codeword (1, 0, 1, 1) and the detected results. It can be seen that the distance is minimized by decoding the codeword



as  $(0, 0, 0, 1)$ , which represents data bits ‘00’.



## 5.3 Numerical Results

In this section we numerically compare the SERs of the coded and uncoded scenarios under different decoding criteria for TM scenario of both active and passive transport systems. The simulation parameters are set to be the same as the OOK systems for molecules type  $A$ ,  $B$ , and  $C$ : the diffusion coefficient  $D = 10^{-6}$  cm<sup>2</sup>/s, the distance between the transmitter and the receiver  $d = 20$  μm, and the drift velocity  $v = 2$  μm/s in active transport. The channel codes used for simulations are also  $[4, 2]$  block codes, which means that there are  $\binom{2^4}{4} = 1820$  possible codebook selections. The joint coding-modulation we mentioned in Section 2.4 is applied, and the actual coded transmission pattern for each symbol has 2 bits rather than 4 bits as the OOK system because each molecule of type  $A$ ,  $B$ , and  $C$  represents two coded bits. There are  $4^{64}$  decoding rules for each codebook selection, where the 4 means 4 codewords for a codebook, and the 64 means  $(2^2)^3$  for 3 types of molecule and the  $2^2$  for 4 possible decomposed codeword patterns  $\{(0, 0), (0, 1), (1, 0), (1, 1)\}$ . When calculating the probability-based distance, we use  $N = 2$ . In order to compare the uncoded and coded scenario fairly, we use the same average bit duration  $T$ , which is the average period to send one information bit.

### 5.3.1 Active Transport via Brownian Motion with Drift

In Fig. 5.2, we show the SER distribution over all codebooks under different decoding rules for TM systems when  $T = 100$  s. We compare the minimum distance decoding rules of using the probability-based distance, the pattern-based distance, and the Hamming distance, along with using the optimal decoding rule. The codebooks are then indexed by the order of descending SER using the optimal decoding rule. Similar to the case of OOK systems, we see that most of the codebooks do not lead to better performance than the uncoded system, and there are only 60, 38 and 37 codebooks that result in better performance than the uncoded system when using the optimal decoding rule, MD decoding

with the probability-based distance and the pattern-based distance, respectively. The SER of the uncoded scenario is 0.24%. The SERs of the best codebook are 0.11% using the optimal decoding rule, 0.11% using the MD decoding with the probability-based distance, 0.11% using the MD decoding with the pattern-based distance, and 0.25% using the MD decoding with the Hamming distance, respectively. When the Hamming distance is used as the MD decoding rule, all codebooks result in worse performance than the uncoded system.

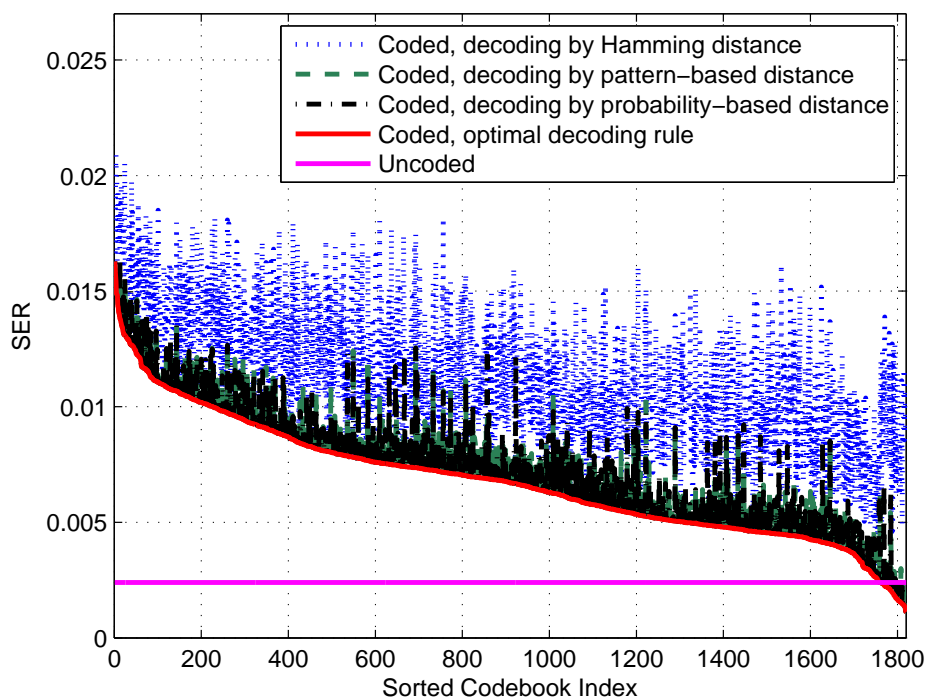


Figure 5.2: SER distribution under different decoding rules for TM systems with  $T = 100$  s. The codebooks are indexed by the order of descending SER using the optimal decoding rule.

The SER performances of the TM system under various  $T$  using the optimal decoding rule, the MD decoding with the probability-based distance, the pattern-based distance, and the Hamming distance are shown in Fig. 5.3. The results of the uncoded scenario are also plotted for reference. We can see that the joint coding-modulation scheme can effectively lower the SER. Both the probability-based distance and the pattern-based distance is overlapped with the optimal decoding rule, showing the effectiveness of the proposed distances. Compared to the OOK system (Fig. 4.3), the SERs for the TM system are at

least an order lower, meaning that using multiple types of molecules (if they are available) can greatly improve the system performance.

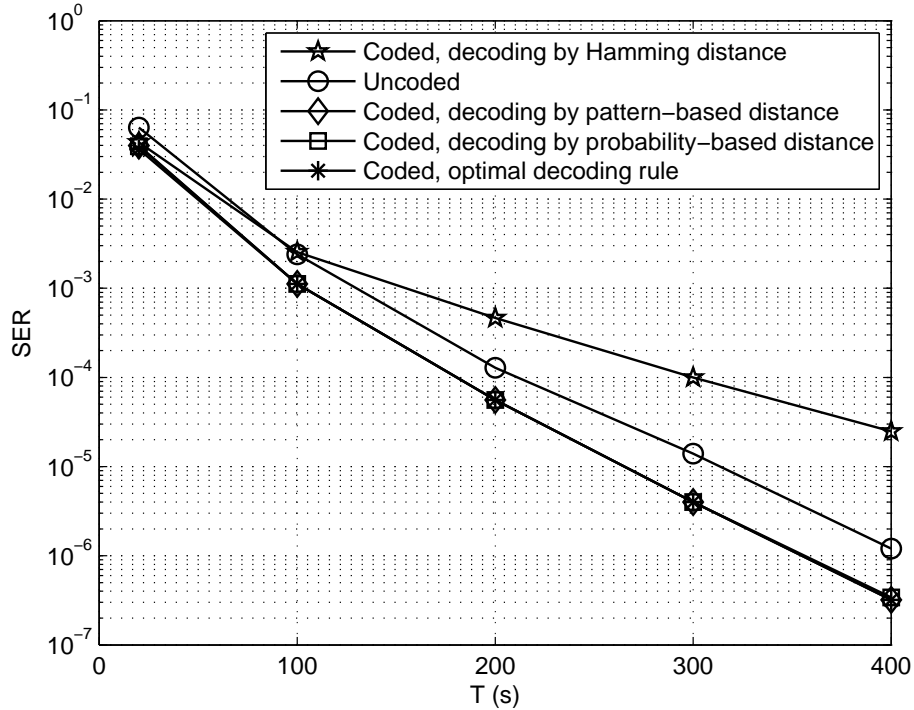
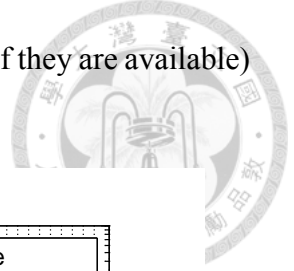


Figure 5.3: Comparison of SER performances for the uncoded TM system and the coded TM systems employing optimal decoding rule, MD decoding with probability-based distance, MD decoding with pattern-based distance, and MD decoding with Hamming distance.

To understand more about the proposed distances, and the Hamming distance, we compare their performances with the optimal decoding rule under different  $T$ . In Fig. 5.4, we show the amount of codebooks decoding by MD with the three distances performing exactly as the optimal decoding rule. We can see that the amount of codebooks grow from about 100 to 700 when  $T$  grows from 20 s to 400 s for both the probability-based distance and the pattern-based distance. When  $T$  is larger than 300 s, the pattern-based distance even has slightly more codebooks with the same performance as the optimal decoding rule than the probability-based distance, showing that in the case of the TM active transport system, the method of summing crossover levels used in the pattern-based distance for approximating the actual channel coding distance between codewords is more optimal. The cases of decoding with the Hamming distance are much worse and thus not suitable for decoding in active transport, and there are only about 50 codebooks performing as the

optimal decoding rule.

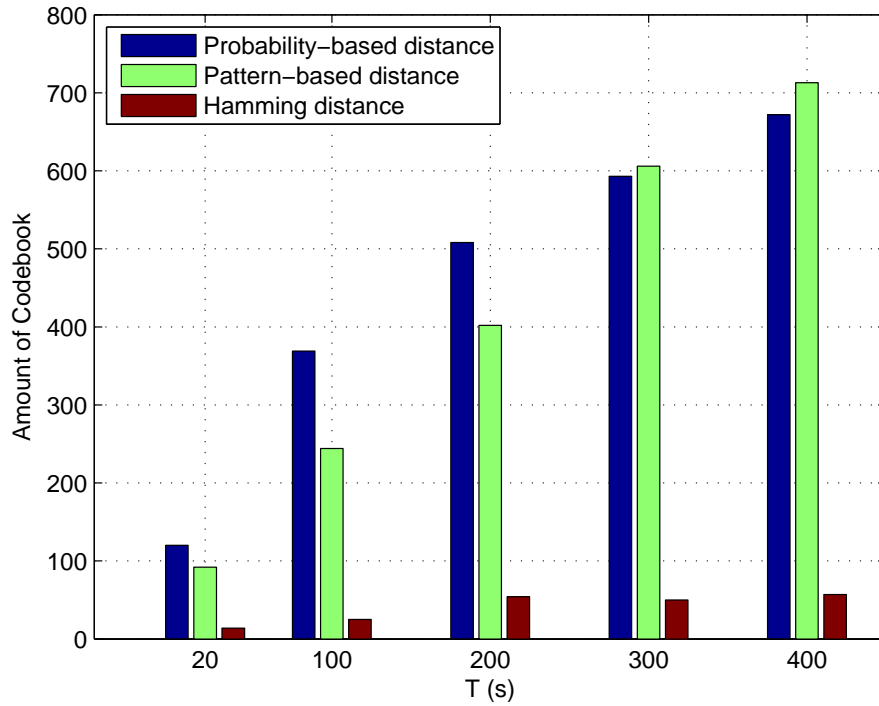
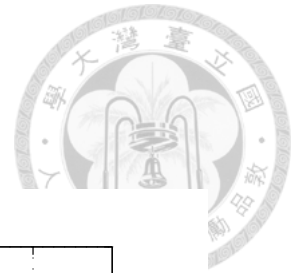


Figure 5.4: The amount of codebooks decoding by MD with the probability-based, the pattern-based, and the Hamming distance having the same performance as the optimal decoding rule under different  $T$  for TM systems.

As shown in Fig. 5.5, we compare the performance between the probability-based, the pattern-based, and the Hamming distance, and shows the amount of codebook about decoding by which distance would have the best SER performance among the three distances. We can see that the probability-based distance outperforms other distances with having approximately 1400 codebooks performing the best among all cases of  $T$ . The pattern-based distance catches up with growing from 700 codebooks, and reaching to 1500 codebooks when  $T = 400$  s. The Hamming distance has only about 100 codebooks having the lowest SER. We conclude that the probability-based distance leads to better results in most practical cases, and when  $T$  is larger than 300 s, the pattern-based distance performs as good. Therefore, we suggest decoding with the probability-based distance when  $T \leq 300$  s, and switch to the pattern-based distance when  $T$  is larger.

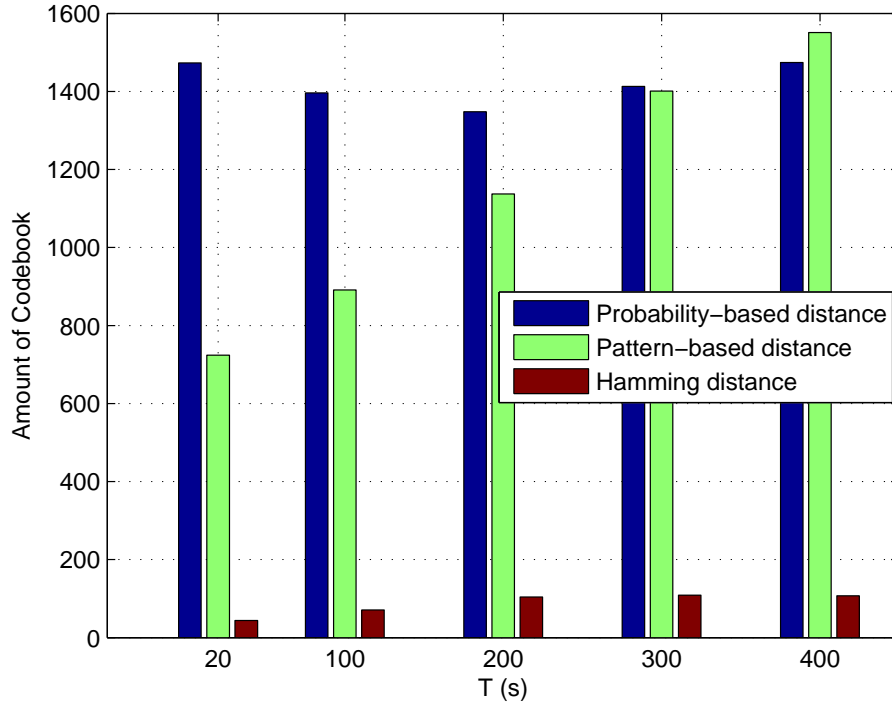


Figure 5.5: The amount of codebook performing the best among MD decoding with the probability-based, the pattern-based, and the Hamming distance under different  $T$  for TM systems.

### 5.3.2 Passive Transport via Brownian Motion

In Fig. 5.6, we show the SER distribution over all codebooks under different decoding rules for TM systems when  $T = 100$  s. We compare the minimum distance decoding rules of using the probability-based distance, the pattern-based distance, and the Hamming distance, along with using the optimal decoding rule. The codebooks are indexed by the order of descending SER using the optimal decoding rule. There are 951 codebooks decoding with the optimal decoding rule performing better than the uncoded system. The best SERs are 4.25% using the optimal decoding rule, 4.68% using the MD decoding with the Hamming distance, 4.33% using the MD decoding with the probability-based distance, and 4.64% using the MD decoding with the pattern-based distance, respectively; while the SER is 8.96% for the uncoded scenario. We can see from Fig. 5.6 that the performance of the SER decoding with Hamming distance is worse than the case with the probability-based for passive transport. The comparison between the Hamming distance and the pattern-based distance can't be clearly observed in Fig. 5.6, and we will further

discuss the comparison between them later in this subsection.

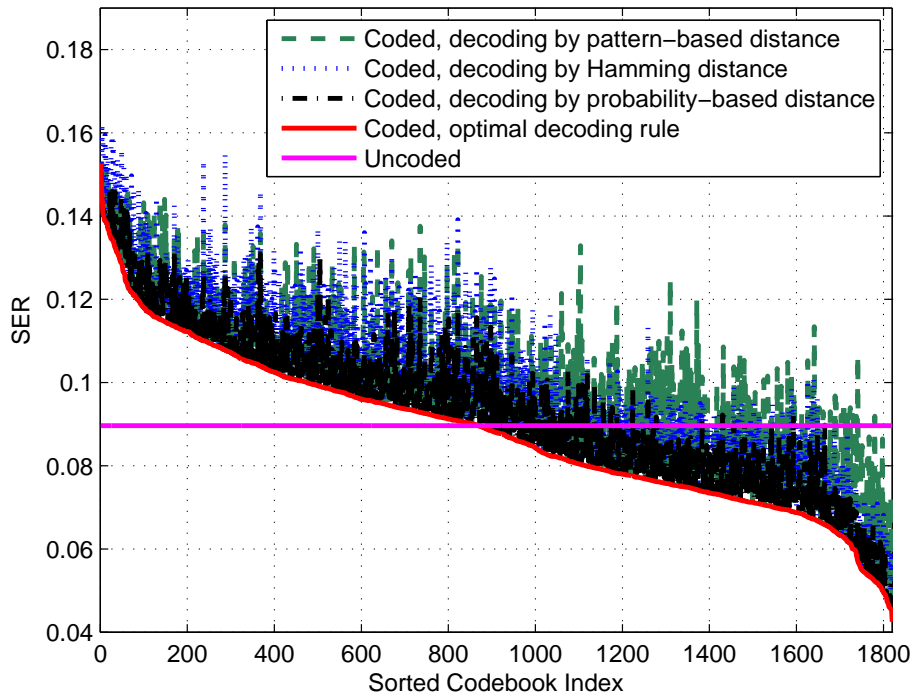


Figure 5.6: SER distribution under different decoding rules for TM systems with  $T = 100$  s. The codebooks are indexed by the order of descending SER using the optimal decoding rule.

The SER performances of the type-based modulation system under various  $T$  using the MD decoding with the probability-based distance, the pattern-based distance, the Hamming distance are shown in Fig. 5.7. The results of the uncoded scenario and the results of using the optimal decoding rule are also plotted for reference. We can see that the joint coding-modulation scheme can effectively lower the SER. The SER results of the Hamming distance is slightly worse than the probability-based distance and the pattern-based distance. However, the Hamming distance has the advantage of low computational complexity; therefore, choosing the Hamming distance or the probability-based and the pattern-based distance can be considered a tradeoff between SER performance and computational complexity. Compared to the OOK system (Fig. 4.7), the SERs for the TM system are lower for about half an order, meaning that using multiple types of molecules (if they are available) can greatly improve the system performance.

Parallel to the OOK system, we compare the performances of the probability-based

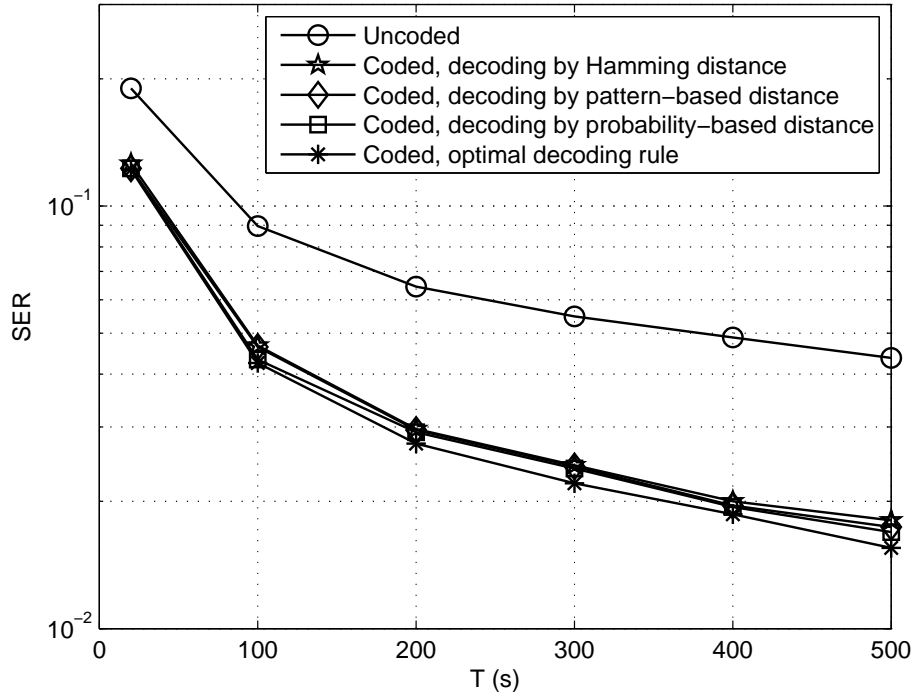


Figure 5.7: Comparison of SER performances for the uncoded TM system and the coded TM systems employing optimal decoding rule, MD decoding with probability-based distance, MD decoding with pattern-based distance, and MD decoding with Hamming distance.

distance, the pattern-based distance, and the Hamming distance with the optimal decoding rule under different bit duration  $T$  to understand more about the performance comparison between the distances. In Fig. 5.8, we show the number of codebooks decoding by MD with the probability-based, the pattern-based, and the Hamming distance performing having the same performance as the optimal decoding rule.

There are about 70, 50 and 15 codebooks having the same performance as the optimal decoding in the case of decoding by the probability-based distance, the pattern-based distance and the Hamming distance, respectively. We can see that more codebooks have the same performance as the optimal decoding in the case of decoding by the probability-based distance. Although the codebook amount of having the same performance as the optimal decoding rule is lower than the OOK system, we can see from Fig. 5.7 that the SER results of the distances are still close to the SER of the optimal decoding rule.

Similarly, we compare the performance between the probability-based, the pattern-based, and the Hamming distance, and shows the amount of codebook about decoding

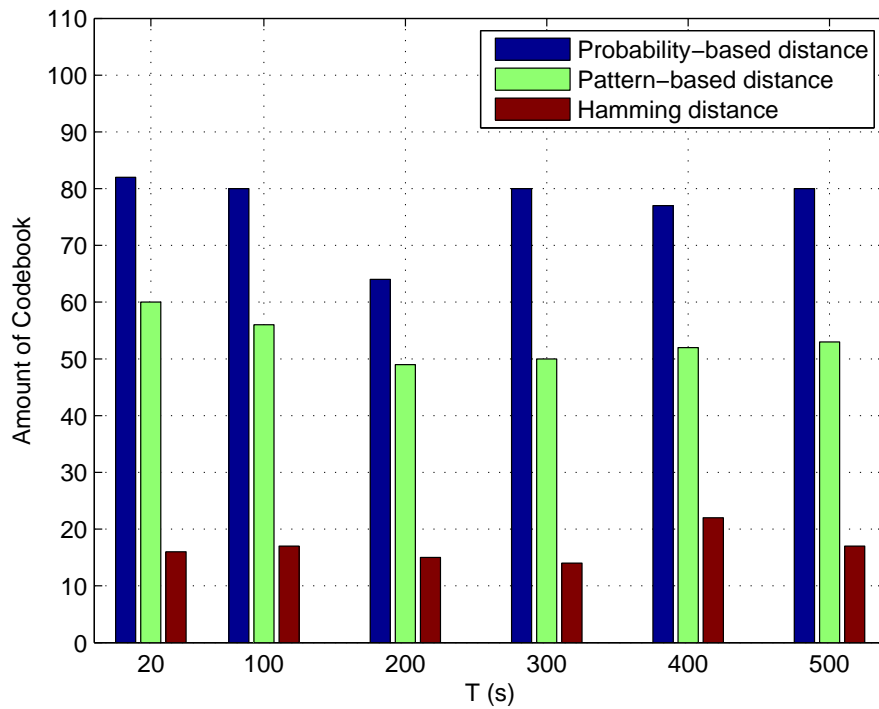


Figure 5.8: The amount of codebooks decoding by MD with the probability-based, the pattern-based, and the Hamming distance performing having the same performance as the optimal decoding rule under different  $T$  for TM systems.

by which distance would have the best SER performance among the three distances in Fig. 5.9. We can see that the probability-based distance as well outperforms other distances with having more than 1200 codebooks performing the best among all cases of  $T$ . About 450 codebooks perform better with decoding by the pattern-based distance than the Hamming distance (about 300 codebooks.) Like the scenario of OOK system, the probability-based distance leads to better results in most practical cases. Note that, however, the pattern-based distance and the Hamming distance have the advantage of low computational complexity. Therefore, choosing the probability-based distance, the pattern-based distance, or the Hamming distance can be considered a tradeoff between SER performance and computational complexity.



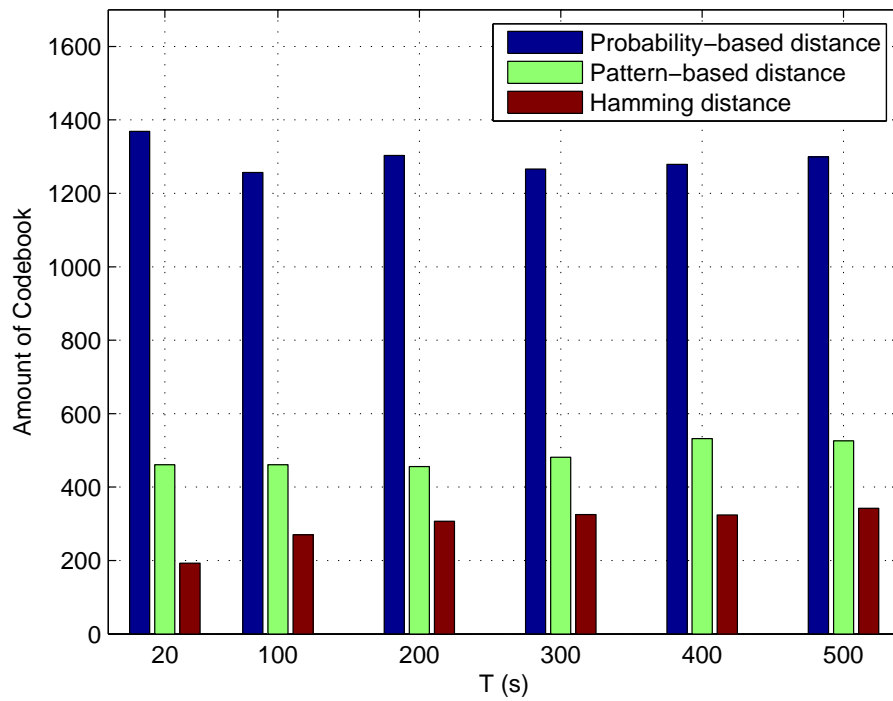


Figure 5.9: The amount of codebook performing the best among MD decoding with the probability-based, the pattern-based, and the Hamming distance under different  $T$  for TM systems.



## Chapter 6

# Conclusions and Future Research

In this thesis, we have examined the idea of adopting channel coding for diffusion-based molecular communications. We have proposed two categories of distance functions, the *probability-based distance* and the *pattern-based distance*, for diffusion-based molecular communication systems. Numerical results have shown that the proposed distance functions are more suitable as channel code design metrics for diffusion channels and the proposed distance functions lead to much better SER performance when used as minimum distance decoding rule than the traditionally used Hamming distance.

In both on-off keying (OOK) and synchronous type-based modulation (TM) for active transport, the SER results decoding with our proposed distances for minimum distance decoding is nearly identical to using the optimal decoding rule, and significantly outperforms the Hamming distance for channel decoding. None of the cases decoding with the Hamming distance performs better than the uncoded scenario, showing that the traditional Hamming distance is no longer a good distance function. Since the probability-based distance results in better performance than the pattern-based distance in most practical cases while the pattern-based distance has the advantage of lower computational complexity, choosing the probability-based distance or the pattern-based distance can be considered a tradeoff between SER performance and computational complexity.

Channel coding in passive transport can improve the SER performance more than in the case of active transport. In OOK systems of the passive transport, the SERs of the best performance codebook for the probability-based, the pattern-based and the Hamming dis-

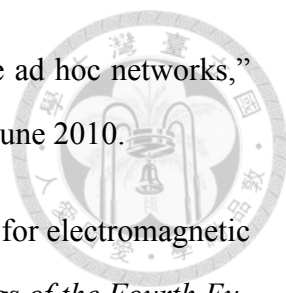
tance is similar, and there are more codebooks decoding by the probability-based distance perform as well as the optimal decoding. The SER results decoding with the Hamming distance performs slightly worse than than the cases with the proposed distances in TM systems for passive transport. Channel coding can indeed improve the symbol error rate (SER) results when encoding with proper codebooks and decoding with suitable distance functions.

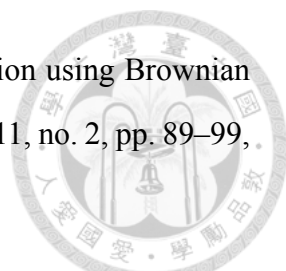
The effort in our work serves as a beginning study of a brand new channel coding concept for diffusion-based molecular communications. The concept mentioned in this thesis can be applied to any diffusion-based channel if the delay distribution is known. The work can also be extended for other cases of level-based and type-based modulation schemes in diffusion-based molecular communications. More scenarios can be considered, such as applying different channel coding methods or taking the constraint of molecular amount into consideration. Using the two proposed distance functions to design suitable codebooks will also be discussed as a future work.

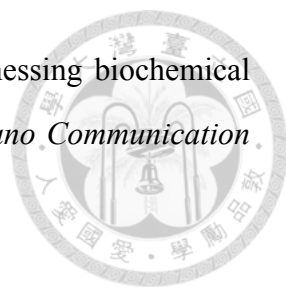


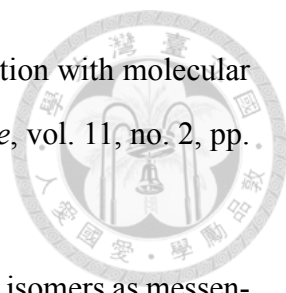
## Bibliography

- [1] I. F. Akyildiz, F. Brunetti, and C. Blázquez, “Nanonetworks: A new communication paradigm,” *Computer Networks (Elsevier) Journal*, vol. 52, no. 11, pp. 2260–2279, Aug. 2008.
- [2] I. Llatser, E. Alarcón, and M. Pierobon, “Diffusion-based channel characterization in molecular nanonetworks,” in *Proc. IEEE Conference on Computer Communications Workshops (INFOCOM WKSHPs)*. IEEE, 2011, pp. 467–472.
- [3] R. Freitas, “Nanotechnology, nanomedicine and nanosurgery,” *International Journal of Surgery*, vol. 3, no. 4, pp. 243–246, 2005.
- [4] J. Han, J. Fu, and R. B. Schoch, “Molecular sieving using nanofilters: past, present and future,” *Lab on a Chip*, vol. 8, no. 1, pp. 23–33, 2008.
- [5] C. M. Pieterse and M. Dicke, “Plant interactions with microbes and insects: from molecular mechanisms to ecology,” *Trends in plant science*, vol. 12, no. 12, pp. 564–569, 2007.
- [6] H. Dai, “Carbon nanotubes: synthesis, integration, and properties,” *Accounts of chemical research*, vol. 35, no. 12, pp. 1035–1044, Aug. 2002.
- [7] T. Suda, M. Moore, T. Nakano, R. Egashira, and A. Enomoto, “Exploratory research on molecular communication between nanomachines,” in *Genetic and Evolutionary Computation Conference (GECCO), Late Breaking Papers*, Jun. 2005.
- [8] M. S. Islam and L. VJ, “Nanoscale materials and devices for future communication networks,” in *IEEE Communications Magazine*, vol. 48, Jun. 2010, pp. 112–120.

- 
- [9] B. Atakan and O. B. Akan, “Carbon nanotube-based nanoscale ad hoc networks,” *IEEE Communications Magazine*, vol. 48, no. 6, pp. 129–135, June 2010.
- [10] J. M. Jornet and I. F. Akyildiz, “Graphene-based nano-antennas for electromagnetic nanocommunications in the terahertz band,” in *2010 Proceedings of the Fourth European Conference on Antennas and Propagation (EuCAP)*, April 2010, pp. 1–5.
- [11] R. Freitas, *Nanomedicine, Volume I: Basic Capabilities*. Landes Bioscience, 1999.
- [12] S. Hiyama, Y. Moritani, T. Suda, R. Egashira, A. Enomoto, M. Moore, and T. Nakano, “Molecular communication,” *Proc. 2005 NSTI Nanotechnology Conference*, vol. 3, pp. 391–394, 2005.
- [13] B. Alberts, D. Bray, K. Hopkin, A. Johnson, J. Lewis, M. Raff, K. Roberts, and P. Walter, *Essential Cell Biology*. Garland, 2009.
- [14] T. D. Pollard, W. C. Earnshaw, and J. Lippincott-Schwartz, *Cell Biology*. Saunders, 2007.
- [15] N. Farsad, A. W. Eckford, S. Hiyama, and Y. Moritani, “On-chip molecular communication: analysis and design,” *IEEE Transactions on NanoBioscience*, vol. 11, no. 3, pp. 304–314, Sep. 2012.
- [16] P.-C. Yeh, K.-C. Chen, Y.-C. Lee, L.-S. Meng, P.-J. Shih, P.-Y. Ko, W.-A. Lin, and C.-H. Lee, “A new frontier of wireless communications theory: Diffusion-based molecular communications,” *IEEE Wireless Communications Magazine*, vol. 19, no. 5, pp. 28–35, Oct. 2012.
- [17] A. Einstein, “On the movement of small particles suspended in stationary liquids required by the molecular-kinetic theory of heat,” *Annalen Der Physik*, vol. 17, pp. 549–560, 1905.
- [18] A. Eckford, “Nanoscale communication with Brownian motion,” in *Proc. 41st Ann. Conf. Inform. Sci. Syst.*, March 2007, pp. 160–165.

- 
- [19] S. Kadloor, R. Adve, and A. Eckford, “Molecular communication using Brownian motion with drift,” *IEEE Transactions on NanoBioscience*, vol. 11, no. 2, pp. 89–99, June 2012.
- [20] H. C. Berg, *Random Walks in Biology*. Princeton University Press, NJ, USA., 1993.
- [21] T. Nakano, T. Suda, M. Moore, R. Egashira, A. Enomoto, and K. Arima, “Molecular communication for nanomachines using intercellular calcium signaling,” in *Proc. 5th IEEE Conference on Nanotechnology*, vol. 2, Jul. 2005, pp. 478–481.
- [22] D. E. Clapham, “Calcium signaling,” *Cell*, vol. 131, pp. 1047–1058, Dec. 2007.
- [23] T. Nakano and J. Liu, “Design and analysis of molecular relay channels: an information theoretic approach,” *IEEE Transactions on NanoBioscience*, vol. 9, no. 3, pp. 213–221, Sep. 2010.
- [24] M. Moore, T. Suda, and K. Oiwa, “Molecular communication: Modeling noise effects on information rate,” *IEEE Transactions on NanoBioscience*, vol. 8, no. 2, pp. 169–180, June 2009.
- [25] P.-J. Shih, C.-H. Lee, and P.-C. Yeh, “Channel codes for mitigating intersymbol interference in diffusion-based molecular communications,” in *Proc. IEEE GLOBECOM*, Dec. 2012, pp. 4228–4232.
- [26] P.-J. Shih, C.-H. Lee, P.-C. Yeh, and K.-C. Chen, “Channel codes for reliability enhancement in molecular communication,” to appear in *IEEE Journal on Selected Areas in Communications*, 2013.
- [27] K. V. Srinivas, A. Eckford, and R. Adve, “Molecular communication in fluid media: The additive inverse gaussian noise channel,” *IEEE Transactions on Information Theory*, vol. 58, no. 7, pp. 4678–4692, July 2012.
- [28] K. R. Sharma, *Principles Of Mass Transfer*. Prentice-Hall Of India Pvt. Limited, 2007.

- 
- [29] S. Hiyama and Y. Moritani, “Molecular communication: harnessing biochemical materials to engineer biomimetic communication systems,” *Nano Communication Networks*, vol. 1, no. 1, pp. 20–30, 2010.
- [30] S. Karlin and H. Taylor, *A First Course in Stochastic Processes*. Academic Press, 1975.
- [31] R. S. Chhikara and J. L. Folks, *The inverse gaussian distribution: theory, methodology, and applications*. New York, NY, USA: Marcel Dekker, Inc., 1989.
- [32] L.-S. Meng, P.-C. Yeh, K.-C. Chen, and I. F. Akyildiz, “A diffusion-based binary digital communication system,” in *Proc. IEEE International Conference on Communications (ICC)*, June 2012, pp. 4985–4989.
- [33] J. P. Nolan, *Stable Distributions - Models for Heavy Tailed Data*. Boston: Birkhauser, 2015, in progress, Chapter 1 online at [academic2.american.edu/~jpnolan](http://academic2.american.edu/~jpnolan).
- [34] S. M. Ross, *Introduction to Probability Models, 9th ed.* Academic Press, 2006.
- [35] Y.-P. Hsieh, Y.-C. Lee, P.-J. Shih, P.-C. Yeh, and K.-C. Chen, “On the asynchronous information embedding for event-driven systems in molecular communications,” *Nano Communication Networks*, vol. 4, no. 1, pp. 2 – 13, March 2013.
- [36] M. U. Mahfuz, D. Makrakis, and H. T. Mouftah, “A comprehensive study of concentration-encoded unicast molecular communication with binary pulse transmission,” in *Proc. IEEE Conference on Nanotechnology (IEEE-NANO)*, Aug. 2011, pp. 227–232.
- [37] A. W. Eckford, “Achievable information rates for molecular communication with distinct molecules,” in *Proc. Bio-Inspired Models of Network, Information and Computing Systems (BIONETICS)*, Dec. 2007, pp. 313–315.

- 
- [38] B. Atakan, S. Galmes, and O. B. Akan, “Nanoscale communication with molecular arrays in nanonetworks,” *IEEE Transactions on NanoBioscience*, vol. 11, no. 2, pp. 149–160, June 2012.
- [39] N.-R. Kim and C.-B. Chae, “Novel modulation techniques using isomers as messenger molecules for molecular communication via diffusion,” in *Proc. IEEE International Conference on Communications (ICC)*. IEEE, June 2012, pp. 6146–6150.
- [40] M. S. Kuran, H. B. Yilmaz, T. Tugcu, and I. F. Akyildiz, “Modulation techniques for communication via diffusion in nanonetworks,” in *Proc. IEEE International Conference on Communications (ICC)*. IEEE, June 2011, pp. 1–5.
- [41] P.-Y. Ko, Y.-C. Lee, P.-C. Yeh, C.-H. Lee, and K.-C. Chen, “A new paradigm for channel coding in diffusion-based molecular communications: Molecular coding distance function,” in *Proc. IEEE GLOBECOM*, Dec. 2012, pp. 3772–3777.
- [42] Y.-P. Hsieh, P.-J. Shih, Y.-C. Lee, P.-C. Yeh, and K.-C. Chen, “An asynchronous communication scheme for molecular communication,” in *Proc. International Workshop on Molecular and Nanoscale Communications (ICC’12 WS - MoNaCom)*, June 2012, pp. 7755–7760.